Barrier crossing with concentration boundary conditions in biological channels and chemical reactions

Victor Barcilon
Departments of The Geophysical Sciences and Mathematics, University of Chicago, Chicago, Illinois 60637

Duanpin Chen and Robert S. Eisenberg
Department of Physiology, Rush Medical College, Chicago, Illinois 60612

Mark A. Ratner
Department of Chemistry, Northwestern University, Evanston, Illinois 60208

(Received 4 May 1992; accepted 30 September 1992)

Ions move into biological cells through pores in proteins called ionic channels, driven by gradients of potential and concentration imposed across the channel, impeded by potential barriers and friction within the pore. It is tempting to apply to channels the chemical theory of barrier crossing, but important issues must first be solved: Concentration boundary conditions must be used and flux must be predicted for applied potentials of all sizes and for barriers of all shapes, in particular, for low barriers. We use a macroscopic analysis to describe the flux as a convolution integral of a mathematically defined adjoint function, a Green's function. It so happens that the adjoint function also describes the first-passage time of a *single* particle moving between boundary conditions *independent of concentration*. The (experimentally observable) flux is computed from analytical formulas, from simulations of discrete random walks, and from simulations of the Langevin or reduced Langevin equations, with indistinguishable results. If the potential barrier has a single, large, parabolic peak, away from either boundary, an approximate expression reminiscent of Kramers' formula can be used to determine the flux. The fluxes predicted can be compared with measurements of current through single channels under a wide range of experimental conditions.

I. INTRODUCTION

A. Overview

How can we compute, by means of Langevin simulations, the flux of Brownian particles from one region with concentration c_L to another with concentration c_R? The question is disconcerting since concentration does not appear in the Langevin equation, which describes the motion of a single particle. The apparent answer, "multiply by the concentration," is not adequate, because it is vague: What function should be multiplied by what concentration? This paper answers the question with some degree of mathematical rigor. It shows how to incorporate concentration boundary conditions into Langevin simulations.

This question arises in the study of biological channels, where concentration boundary conditions are unavoidable. An overview of the biological system is given in the next subsection. As explained there, ions diffuse and drift through an aqueous pore in a protein (itself embedded in a membrane) as they move from a bath of one concentration to a bath with another concentration. These ionic motions can be viewed as a barrier crossing problem, similar to that of bimolecular chemical reactions in which a system point traverses a barrier along a reaction coordinate.

Lately, barrier crossing has been studied by simulating the trajectories of individual particles with one of the techniques of molecular dynamics. Molecular dynamics is now a standard tool for analyzing classical processes, both in condensed phase and in vapor. Once interatomic potentials and polarization effects are accurately specified, molecular dynamics is essentially an exact technique on the time scale in which trajectories can be accurately computed. There are, however, certain systems in which molecular dynamics has serious limitations. These include systems (such as ions in channels), whose evolution is studied over time scales very long compared to the propagation time of molecular dynamics, and systems (such as ions in channels) that consist of a subsystem of primary dynamical interest, with the remainder of the system acting largely as a heat bath. For the channel problem, the extended (microsecond) biological time scale and the importance of long range electrostatic forces (including polarization across the entire length of the channel and membrane[1]) suggest that molecular dynamics is not an appropriate or useful computational scheme, by itself. An obvious remedy is to extend molecular dynamics with Langevin simulations.[2]

The barrier crossing problems of biology and chemistry differ in subtle and important ways: (1) The barriers are usually low so that ions flow efficiently and thus perform their biological function of carrying flux or current; (2) the biological output (and experimental observable) is usually the current, sometimes the flux through the channel; (3) the system is essentially one dimensional, so the reaction coordinate is physically clear, and does not re-

 0021-9606/93/021193-20$06.00

quire redefinition (say in terms of steepest descents), rigorously or metaphorically; (4) the masses are also obvious. Despite these differences, we want to stress here the similarity between the two systems.

The chemical literature does not seem to contain any explicit discussion of concentration boundary conditions for Langevin simulations, except for extended quasicrystalline systems, such as diffusion along surfaces or ionic motion through solid electrolytes, where periodic boundary conditions are used. Clearly, such periodic boundary conditions cannot be used to describe the flux through biological channels, which depends on the difference in concentrations between the boundaries.

The general thrust of our analysis is as follows. First we switch from a reduced Langevin description of the problem to a Smoluchowski description for which concentration boundary conditions can be rigorously enforced. Next, we introduce an adjoint problem in order to derive a general formula for the flux; the solution of this adjoint problem serves as a Green's function relating the output flux to the input concentrations. Then, we give a probabilistic interpretation to this adjoint problem: It describes the distribution of the first-passage time *of a single particle* moving over the same barrier but with very specific boundary conditions, independent of concentration, namely, an exit absorbing boundary through which the particle escapes and is counted and an entrance absorbing boundary through which the particles escapes uncounted. Finally, now that this central, well-defined stochastic problem for a single particle has been uncovered, we close the loop by performing Langevin simulations of single particle motions with the single-particle boundary conditions just derived.

The previous paragraph is a brief outline of the paper, in particular, Secs. II, III, IV, and VII. The rest of this Introduction summarizes some of the biological features of channels. In Secs. V and VI we go from a Smoluchowski description back to a reduced Langevin equation. In Sec. IX we examine the case of an Eckart potential to test the accuracy of our simulation technique, while Sec. VIII considers the case of a single high barrier, and contrasts our results to the classical paper of Kramers (1940).

B. Biological channels

Biological membranes are punctured by proteins that allow the flow of ions in and out of cells. Ions moving through these protein channels are responsible for many processes of biological interest[3,4] such as secretion of hormones, coordination of muscle contraction, and information transmission and processing in the nervous system. Each channel type is characterized by the amount of current that flows when it is open and, to a lesser extent, by open channel noise, namely, the fluctuations from the mean value of open current. Different channel types have open amplitudes ranging from immeasurable (say, less than 100 fA) to nearly 1 nA. The duration of openings varies almost as widely, ranging from less than 10 μs to seconds. Experimentally, the channel record is an electrical signal of the flux of charged particles (often predominantly cations) through the channel. The channel problem can be idealized as current flow through a one-dimensional pore, with boundary conditions corresponding to different concentrations at each end, with the pore subject to some electrical potential. The problem for the theorist, then, is to compute the flux across such a channel and compare it to the experimental record.

The motion of ions in channels is likely to be governed by (1) the random collisions with the surrounding water molecules and channel protein; (2) the interaction with other nearby ions; and (3) the electric fields, induced and permanent, which exist in the channel. Because such motions are too difficult to analyze directly, various simplifications have been made. One useful approach replaces the fast time scale (picosecond) collision processes between ions and solvent by a diffusion picture. With this simplification, the viewpoint becomes macroscopic and deterministic: Each ion species is characterized by a concentration $c_i(x,t)$ (units: cm^{-3}). Conservation of species requires that

$$\frac{\partial c_i}{\partial t}+\nabla\cdot\mathbf{J}_i=0, \tag{1.1}$$

where $\mathbf{J}_i$ is the flux of the ith ion (units: $\mathrm{cm}^{-2}\,\mathrm{s}^{-1}$). The physics of the problem enters in the constitutive equation which relates this flux to gradients of concentrations and electric potential, namely,

$$\mathbf{J}_i=-D_i\left(\nabla c_i+\frac{Z_i e}{kT}c_i\nabla\phi\right), \tag{1.2}$$

where D_i is the diffusion coefficient of the ith species (units: $\mathrm{cm}^2\,\mathrm{s}^{-1}$), Z_i its charge number, e the proton charge, k Boltzmann's constant, T the absolute temperature, and finally ϕ is the electric potential.

In certain studies, $\phi(x)$ is taken as given, its features being characteristic of the channel under consideration. In some other studies,[1,5] $\phi(x)$ is determined via the electrostatic version of Maxwell's equations.[6] In these approaches, the potential interacts with the ion distribution inside and on both ends of the channel.

The macroscopic-deterministic approach described above is subject to obvious criticism. A stochastic process is essentially made to appear deterministic by averaging over the long-time resolution of the measuring devices. As measuring devices become faster and faster, the averaging will become less and less justifiable. Indeed, existing measurements already display stochastic features absent from deterministic analyses.

Clearly, there is a need to examine the problem of ion flow through channels from the microscopic, stochastic viewpoint. We adopt an alternate route: We shall track the motion of a single ion via a Langevin-type equation. Many issues in the standard Langevin approach[7-11] need to be clarified before it can be used to analyze flux through ionic channels. For instance, the crucial effect of different concentrations on either side of the channel is not described by traditional Langevin equations.

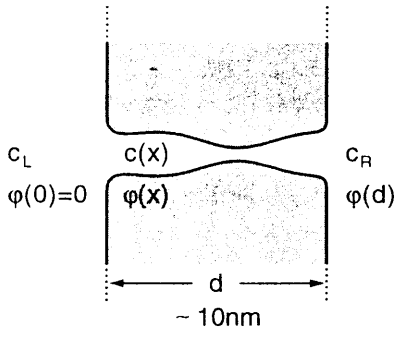

FIG. 1. Sketch of an ionic channel. Note the nearly one-dimensional structure, and the fixed concentrations of ions on each end.

II. THE ONE DIMENSIONAL FLUX FORMULA

In this section we consider the flux problem as a boundary value problem. The approach is a mathematical one gaining in validity what it loses in familiarity. We derive a flux formula for diffusion in a potential $\phi(x)$, subject to appropriate concentration boundary conditions. We shall restrict our attention to one dimensional problems because biological channels are mostly long and narrow (as shown in Fig. 1). Mathematically, the channel is described by partial differential equations (written here using the subscript notation for partial derivatives) with a single spatial variable x,

$$\begin{aligned} &c_t+J_x=0, \\ &J=-D\left(c_x+\frac{Ze}{kT}c\phi_x\right) \end{aligned} \tag{2.1}$$

or to simplify the writing

$$\begin{aligned} &c_t+J_x=0, \\ &J=-Dc_x+\mu c, \end{aligned} \tag{2.2}$$

where

$$\mu(x)=-D\frac{Ze}{kT}\phi_x. \tag{2.3}$$

The potential $\phi(x)$ is arbitrary; it can be fixed by the details of the problem under consideration (in particular, no assumption is made that it contains a barrier large compared to kT, though that limiting case will be considered in Sec. VIII). Given this potential, our goal is to find the concentration and flux of ions. Since the single particle potential is specified at the outset, the different ion species do not interact, and hence we drop the subscripts referring to them, resurrecting them in expressions for the total current carried by all ions, the experimental, observable and biological function of the channel. The different concentrations in the right and left baths are expressed by the boundary conditions

$$\begin{aligned} &c(0,t)=c_L(t), \\ &c(d,t)=c_R(t), \end{aligned} \tag{2.4}$$

where d (units: cm) is the length of the channel.

To complete the description of the problem, we specify the simplest possible initial state, namely,

$$c(x,0)=0. \tag{2.5}$$

The initial condition (2.5) is chosen for convenience. A flux formula for any arbitrary initial concentration can also be derived, and it contains an additional term corresponding to "washout" of the initial contents of the channel. If a continuing source of ions were present within a channel, or chemical system, still another term would appear in the flux formula.

The concentration and flux in the channel at any given time or location can be found by solving the boundary/initial value problem (2.2) with Eqs. (2.4)–(2.5). In particular, solving this problem determines the flux $J(d,\theta)$ at the right end, and at an arbitrary time θ.

Our goal, a Langevin computation of the flux with concentration boundary conditions, is reached by a circuitous path which abandons the direct approach of simply solving Eqs. (2.1)–(2.5). More specifically, we introduce a closely related problem, called the adjoint problem, following the usual practice for solution of (non-self-adjoint) partial differential equations with arbitrary boundary conditions.[12] $J(d,\theta)$ is then written in terms of the solution of this adjoint problem. This circuitous approach is worthwhile because the adjoint turns out to have a precise stochastic interpretation, easily estimated by Langevin simulations, independent of concentration boundary conditions.

To derive the adjoint problem, we multiply the equations in Eq. (2.2) by two functions q^* and k^*, respectively, and integrate these equations over x from 0 to d and over t from 0 to θ. After a few integrations by parts, these equations, when added, read

$$\begin{aligned} &\int_0^\theta dt\int_0^d dx\{c[-q_t^*-(Dk^*)_x-\mu k^*]-J[q_x^*-k^*]\} \\ &+\int_0^d dx\, q^*c\Big|_0^\theta+\int_0^\theta dt\{q^*J+k^*Dc\}\Big|_0^d=0. \end{aligned} \tag{2.6}$$

At this stage, we define the functions q^* and k^* so as to annihilate the double integrals in Eq. (2.6), namely,

$$\begin{aligned} &-q_t^*-(Dk^*)_x-\mu k^*=0, \\ &q_x^*-k^*=0. \end{aligned} \tag{2.7}$$

With these definitions, Eq. (2.6) simplifies considerably

$$\begin{aligned} &\int_0^d dx\, q^*(x,\theta)c(x,\theta)+\int_0^\theta dt\{q^*(d,t)J(d,t) \\ &+k^*(d,t)Dc_R(t)\}-\int_0^\theta dt\{q^*(0,t)J(0,t) \\ &+k^*(0,t)Dc_L(t)\}=0. \end{aligned} \tag{2.8}$$

To derive an expression for the flux at the right end of the channel, we must choose appropriate boundary and initial conditions for q^* and k^*, namely,

$$q^*(x,\theta)=0,$$
$$q^*(d,t)=\delta(\theta-t), \tag{2.9}$$
$$q^*(0,t)=0,$$

so that Eq. (2.8) yields the desired formula. $\delta(\cdot)$ is the Dirac delta "function." With these initial/boundary conditions, which specify q^* and k^* completely, we can write Eq. (2.8) as follows:

$$J(d,\theta)=-\int_0^\theta dt\, k^*(d,t)\,Dc_R(t) + \int_0^\theta dt\, k^*(0,t)\,Dc_L(t). \tag{2.10}$$

Thus the flux at the right end, at an arbitrary time θ can be written in terms of two integrals, which contain the concentrations at either end and the adjoint function k^*.

It is customary to redefine q^* and k^* so they satisfy traditional evolution equations. New adjoint functions are defined by replacing the functions tagged by asterisks with (not tagged) functions depending on the time $\theta-t$; that is to say, from here on the time $\theta-t$ in Eq. (2.9) is replaced by t,

$$q(x,t)=q^*(x,\theta-t),$$
$$k(x,t)=k^*(x,\theta-t). \tag{2.11}$$

Substituting Eq. (2.11) in Eqs. (2.7) and (2.9), we obtain the customary adjoint problem, viz.,

$$q_t=Dk_x+\mu k,$$
$$q_x=k, \tag{2.12}$$

with

$$q(x,0)=0,$$
$$q(0,t)=0, \tag{2.13}$$
$$q(d,t)=\delta(t).$$

The flux formula (2.10) now becomes

$$J(d,\theta)=-\int_0^\theta dt\, k(d,\theta-t)\,Dc_R(t) + \int_0^\theta dt\, k(0,\theta-t)\,Dc_L(t). \tag{2.14}$$

If a nonzero initial condition different from Eq. (2.5) is assumed, or a continuing source is present within the system, additional term(s) enter the flux formula.

For the channel problem with which we are concerned, the bath concentrations c_R and c_L are fixed and the diffusion coefficient D is constant. Therefore, Eq. (2.14) simplifies to

$$J(d,\theta)=-Dc_R\int_0^\theta dt\, k(d,\theta-t)+Dc_L\int_0^\theta dt\, k(0,\theta-t). \tag{2.15}$$

This is our main formula. We should reiterate that so far, our work has merely substituted one way to determine $J(d,\theta)$ with another. The determination of the flux by Eq. (2.14) requires the solution of a problem, viz., the adjoint problem (2.12)–(2.13) for q, which appears to be just as difficult as the original problem (2.2)–(2.5)! However, both because ion concentrations enter explicitly in Eq. (2.15) and because the function q will turn out to describe the probability density of the first-passage time[13] of a *single* particle moving between two absorbing boundaries, the above flux formula will lend itself to several methods of computation.

The steady state version of the flux formula will be needed and is considered next. Even though we could obtain this formula by letting $\theta\to\infty$ in Eq. (2.15), it is preferable to start the derivation *ab initio*. In this case, the governing equations (2.2) reduce to

$$J_x=0,$$
$$J=-Dc_x+\mu c, \tag{2.16}$$

with

$$c(0)=c_L,$$
$$c(d)=c_R. \tag{2.17}$$

Anticipating that moments of $k(x,t)$ and $q(x,t)$ will enter our formula, we define them as

$$\left.\begin{aligned}\mathscr{Q}_n(x)&=\int_0^\infty t^n q(x,t)dt\\ \mathscr{K}_n(x)&=\int_0^\infty t^n k(x,t)dt\end{aligned}\right\}\quad \text{for}\quad n=0,1,2\cdots. \tag{2.18}$$

$\mathscr{Q}_0(x)$ is the probability that a particle starting at x is absorbed at the right end, regardless of the time necessary for this event to happen. $\mathscr{Q}_1(x)$ is the mean time that elapses between the moment the particle leaves x and is absorbed at the right end.

Multiplying Eqs. (2.12)–(2.13) by t and integrating, we see that

$$-n\mathscr{Q}_{n-1}=D\mathscr{K}_n'+\mu\mathscr{K}_n,$$
$$\mathscr{Q}_n'=\mathscr{K}_n, \tag{2.19}$$

with

$$\mathscr{Q}_n(0)=0,$$
$$\mathscr{Q}_n(d)=\delta_{n0}, \tag{2.20}$$

where δ_{n0} is the Kronecker delta. If we multiply the steady-state constitutive equation in Eq. (2.16) by $\mathscr{K}_0$ and integrate over the length of the channel, we get

$$\begin{aligned}J\int_0^d\mathscr{K}_0(x)dx&=\int_0^d(-Dc'+\mu c)\mathscr{K}_0(x)dx\\ &=-Dc\mathscr{K}_0\big|_0^d+\int_0^d(D\mathscr{K}_0'+\mu\mathscr{K}_0)c\,dx\\ &=-Dc_R\mathscr{K}_0(d)+Dc_L\mathscr{K}_0(0).\end{aligned} \tag{2.21}$$

In deriving the steady-state result, we have used the equation for $\mathscr{K}_0$ by setting $n=0$ in Eq. (2.19). To stress the analogy with Eq. (2.15), we rewrite the above result as

$$J=-Dc_R\frac{\mathscr{K}_0(d)}{\int_0^d\mathscr{K}_0(x)dx}+Dc_L\frac{\mathscr{K}_0(0)}{\int_0^d\mathscr{K}_0(x)dx}. \tag{2.22}$$

Finally, if we integrate the second $n=0$ equation in Eq. (2.19), we see that

$$\begin{aligned}\mathscr{Q}_0(x)\,|_0^d&=\int_0^d\mathscr{K}_0(x)dx,\\ 1&=\int_0^d\mathscr{K}_0(x)dx.\end{aligned} \tag{2.23}$$

Therefore, Eq. (2.22) simplifies further and becomes

$$J=-Dc_R\mathscr{K}_0(d)+Dc_L\mathscr{K}_0(0). \tag{2.24}$$

Since $\mathscr{K}_0(x)$ can be written explicitly, viz.,

$$\mathscr{K}_0(x)=\frac{\exp[(Ze/kT)\phi(x)]}{\int_0^d\exp[(Ze/kT)\phi(\xi)]d\xi}, \tag{2.25}$$

we do have an explicit expression for J, which we shall use in Sec. IX. However, the stochastic interpretation of $\mathscr{K}_0(0)$, $\mathscr{K}_0(d)$ will be even more important than Eq. (2.25) and will yield a computational method based upon the statistics of trajectories.

The relationship, if any, between the quantities $\mathscr{K}_0(0)$ and $\mathscr{K}_0(d)$ which enter in the flux formula, and the mean first-passage time $\mathscr{Q}_1(0)$ is not clear to us (but see Ref. 14), particularly given Eq. (2.20). This is in marked contrast to what would be obtained, had we used a different underlying stochastic process, namely, a random walk with a *reflecting* boundary on the left and an absorbing boundary on the right, in which case (see the Appendix) the relationship is simple, well known, and widely used.[15–18]

Although the expression for the steady-state concentration $c(x)$ will not be used here, we record it for the sake of completeness,

$$\begin{aligned}c(x)=&c_R\exp\left[-\frac{Ze}{kT}\{\phi(x)-\phi(d)\}\right]\\&\cdot\frac{\int_0^x\exp[(Ze/kT)\phi(\xi)]d\xi}{\int_0^d\exp[(Ze/kT)\phi(\xi)]d\xi}\\&+c_L\exp\left[-\frac{Ze}{kT}\{\phi(x)-\phi(0)\}\right]\\&\cdot\frac{\int_x^d\exp[(Ze/kT)\phi(\xi)]d\xi}{\int_0^d\exp[(Ze/kT)\phi(\xi)]d\xi}.\end{aligned} \tag{2.26}$$

III. STOCHASTIC INTERPRETATION OF THE ADJOINT PROBLEM: THE DISCRETE CASE

Diffusion problems can generally be viewed as limits of random walks.[19,20] In this section, we interpret the adjoint function q of Eqs. (2.12)–(2.13) as a limit of a probability Q associated with the excursion of a random walker.

Let us consider an interval of length d later identified with the channel. We divide this interval into $N+1$ equal sub-intervals of length Δx. Clearly,

$$(N+1)\Delta x=d. \tag{3.1}$$

Similarly, we discretize the time interval $(0,\theta)$, by introducing $M+1$ time intervals of length Δt. Again we record the fact that

$$(M+1)\Delta t=\theta. \tag{3.2}$$

We shall be concerned in this section with one aspect of the classical random walk of a particle on the spatial lattice $0,\Delta x,2\Delta x,\ldots,(N+1)\Delta x$. The rules governing the random walk are the usual ones, namely, at every generic time interval $m\Delta t$, the particle which is, say, at the generic location $n\Delta x$ has a probability r_n of moving to the right lattice point, a probability l_n of moving to the left lattice point, or a probability $(1-r_n-l_n)$ of staying where it is. The "stay put" probability must be included, if the random walk is to describe a diffusion process in which the diffusion coefficient D is a function of coordinate[21,22] (compare with pp. 208–209 and pp. 213–215 of Ref. 19).

In this section we evaluate the distribution of arrival times. More specifically, we determine the time a particle takes to reach the *right* end point where it contributes to the measured flux. Let $Q_{\alpha,j}$ denote the probability that the particle reaches the right end $x=d$ at time $t=j\Delta t$ *for the first time*, when executing the random walk defined above. The index α indicates that the particle started its journey from $\xi=\alpha\Delta x$. One way to tackle the problem would be to enumerate[23] all the possible trajectories which start at ξ at $t=0$, and end at $x=d$ at $t=j\Delta t$, and compute in this way $Q_{\alpha,j}$; indeed, that is one possible strategy for a simulation. However, analytically it is simpler to derive a difference equation for Q *ab initio*.

Consider a "good" trajectory starting at $\xi=\alpha\Delta x$ and ending at d. After the initial time interval has elapsed, the particle is to be found in one of three locations: $\alpha-1$, α, and $\alpha+1$, with probability l_α, $(1-l_\alpha-r_\alpha)$, and r_α, respectively. From whatever location it is in, the particle has $j-1$ time intervals left to reach the right end point, with respective probabilities $Q_{\alpha-1,j-1}$, $Q_{\alpha,j-1}$, and $Q_{\alpha+1,j-1}$. Therefore,

$$Q_{\alpha,j}=Q_{\alpha-1,j-1}\cdot l_\alpha+Q_{\alpha+1,j-1}\cdot r_\alpha+Q_{\alpha,j-1}\cdot(1-l_\alpha-r_\alpha). \tag{3.3}$$

To this equation we must add boundary and initial conditions. The initial condition is

$$Q_{\alpha,0}=0,\quad\text{for}\quad\alpha=0,1,\ldots,N. \tag{3.4}$$

This initial condition states the obvious, namely, that a particle starting at $\alpha=0,1,\ldots,N$ cannot reach the right end in "no time."

We choose the boundary condition at the left end to be absorbing so that Q will be related to the solution q of the adjoint problem (2.13). As a result, once the particle reaches this left boundary, the random walk stops. In other words,

$$r_0=0. \tag{3.5}$$

Of course, regardless of the boundary condition at the left end, we have

$$l_0\equiv 0. \tag{3.6}$$

As a result, Eq. (3.3) evaluated at $\alpha=0$ implies that

$$Q_{0,j}=Q_{0,j-1},$$

and consequently

$$Q_{0,j}=0, \quad \text{for} \quad j=0,1,\cdots. \tag{3.7}$$

Finally, from the very definition of Q, we can write

$$Q_{N+1,j}=\delta_{j0}. \tag{3.8}$$

To stress the analogy with the adjoint problem, let us rewrite the above problem for Q as a set of two coupled difference equations: we first introduce, as suggested by Eq. (2.12), $K_{\alpha+1/2,j}$ such that

$$K_{\alpha+1/2,j}=\frac{Q_{\alpha+1,j}-Q_{\alpha,j}}{\Delta x}. \tag{3.9a}$$

By introducing this new sequence into the original difference equation (3.3) for Q, we see that

$$Q_{\alpha,j}-Q_{\alpha+1,j}=r_\alpha\cdot\Delta x K_{\alpha+1/2,j-1}-l_\alpha\cdot\Delta x K_{\alpha-1/2,j-1}. \tag{3.9b}$$

To pursue the analogy between Eqs. (3.9a), (3.9b), and (2.12), we must digress a little and discuss the fundamental quantities $\{r_\alpha,l_\alpha\}$ which govern the random walk. To emphasize the distinction between the deterministic and the random components of the walk we write $\{r_\alpha,l_\alpha\}$ as

$$\begin{aligned} r_\alpha&=\frac{s_\alpha}{2}+\frac{\Delta x}{4D}\mu_\alpha,\\ l_\alpha&=\frac{s_\alpha}{2}-\frac{\Delta x}{4D}\mu_\alpha. \end{aligned} \tag{3.10}$$

At this stage, we should view Eq. (3.10) simply as definitions of the quantities s_α and μ_α. Finally, the constant D is just that, namely, a constant. Of course, whenever $r_\alpha\neq l_\alpha$, there is a preference for motion to one side rather than the other. This preferential motion is the "drift" and its strength is related to μ_α, which we shall later identify with the potential gradient. The above formula also implies that as $\Delta x\downarrow 0$ this drift term tends to zero at the same rate as Δx, lest the original hopping rules (3.3) be violated.

Substituting the above expressions in Eqs. (3.9a) and (3.9b), we deduce that

$$\begin{aligned} \frac{Q_{\alpha,j}-Q_{\alpha+1,j}}{\Delta t}&=s_\alpha\frac{(\Delta x)^2}{2\Delta t}\cdot\frac{K_{\alpha+1/2,j-1}-K_{\alpha-1/2,j-1}}{\Delta x}\\ &\quad+\mu_\alpha\frac{(\Delta x)^2}{2D\Delta t}\cdot\frac{K_{\alpha+1/2,j-1}+K_{\alpha-1/2,j-1}}{2},\\ \frac{Q_{\alpha+1,j}-Q_{\alpha,j}}{\Delta x}&=K_{\alpha+1/2,j}. \end{aligned} \tag{3.11}$$

To pursue the analogy with the adjoint problems, we first rewrite the initial condition (3.4) omitting the value $\alpha=0$, viz.,

$$Q_{\alpha,0}=0, \quad \text{for} \quad \alpha=1,\ldots,N \tag{3.12}$$

and boundary conditions (3.7)–(3.8) as

$$\begin{aligned} &Q_{0,j}=0,\\ &Q_{N+1,j}=\delta_{j,0} \end{aligned} \quad \text{for} \quad j=0,1,\cdots. \tag{3.13}$$

Of course, to really make the analogy complete we must pass to the continuous limit. This limiting procedure is outlined briefly in the next section.

IV. THE DIFFUSION LIMIT

In passing to the continuum, several obvious limiting processes must be considered. For instance, we must require that $\Delta x\downarrow 0$ and $\Delta t\downarrow 0$. Of course, this implies that the subintervals are getting smaller and smaller, and consequently, $N,M\to\infty$. These limiting processes are tied in such a way that the products $N\Delta x$ and $M\Delta t$ remain finite, i.e., that Eqs. (3.1)–(3.2) remain in force.

There is, however, a more subtle relation between the above limiting processes. If the random walk is to result in a diffusion process (rather than, say, a wave propagation[24]), then the time step Δt and the spatial step Δx must decrease in such a way that the ratio

$$\frac{(\Delta x)^2}{2\Delta t}\to D, \tag{4.1}$$

where the constant D is the diffusion constant. We shall require this to be the case.

Two other limits must be considered: (1) that of the fundamental sequences r_α,l_α and (2) that of sequences $Q_{\alpha,j},K_{\alpha+1/2,j}$. Returning to Eq. (3.10), we write

$$\begin{aligned} s_n&\to 1,\\ \mu_n&\to\mu(x), \end{aligned} \tag{4.2}$$

where $\mu(x)$ is just a function of x at this stage.

Finally, the probability distribution $Q_{\alpha,j}$ tends to zero in such a way that

$$\frac{Q_{\alpha,j}}{\Delta t}\to q(x,t). \tag{4.3}$$

In other words, Q describes a temporal probability density. Similarly

$$\frac{K_{\alpha+1/2,j}}{\Delta t}\to k(x,t). \tag{4.4}$$

In these formulas, $\alpha\Delta x\to x$ and $j\Delta t\to t$.

With these conditions, the random walk becomes our diffusion process. Indeed, the limit of Eq. (3.11) is

$$\begin{aligned} q_t&=Dk_x+\mu k,\\ q_x&=k, \end{aligned} \tag{4.5}$$

whereas the limits of Eqs. (3.12)–(3.14) are

$$\begin{aligned} q(x,0)&=0,\\ q(0,t)&=0,\\ q(d,t)&=\delta(t). \end{aligned} \tag{4.6}$$

Since Eqs. (4.5)–(4.6) is identical to the adjoint problem (2.11)–(2.12), we can interpret the quantity $q(x,t)dt$ as

the probability that a walker, starting at x, will reach the right end for the first time in the time interval $(t,t+dt)$.

We have reached our goal: We can determine the flux from a bath of one concentration to a bath of another from simulations of the motion of a single particle, in which the concentrations do not enter. The distribution of the first passage time q of the single particle can be found by tracking the motion of an ensemble of random walkers and generating statistics about the trajectories.

The stochastic interpretation of q not only relates the problem to the distribution of first-passage times, but also suggests a counting scheme to compute the flux. Indeed, if we focus on the second term in Eq. (2.14), describing the dependence on c_L, we can say that

$$c_L(t)\Delta x = \text{number of ions in } (0,\Delta x) \text{ at } t. \tag{4.7}$$

Only a small fraction of these ions reach the right end in the time interval $(\theta-t,\theta-t+\Delta\theta)$. The number of such ions is, approximately,

$$\nu(t,\theta) = c_L(t)\Delta x \cdot q\left(\frac{\Delta x}{2},\theta-t\right)\Delta\theta. \tag{4.8}$$

This number is small because the ions are starting their journey very close to an absorbing boundary (but fortunately each of their journeys takes little time to execute or compute). As a result, the probability function $q(\Delta x/2,\theta-t)$ is very small. A Taylor series expansion about $x=0$ yields

$$q(\Delta x/2,\theta-t) = q(0,\theta-t) + q_x(0,\theta-t)\frac{\Delta x}{2} + \cdots \tag{4.8a}$$

or, in view of the boundary condition (4.6)

$$q(\Delta x/2,\theta-t) = q_x(0,\theta-t)\frac{\Delta x}{2} + \cdots \tag{4.8b}$$

which, on account of Eq. (4.5), can be written as

$$q(\Delta x/2,\theta-t) = k(0,\theta-t)\frac{\Delta x}{2} + \cdots. \tag{4.8c}$$

Substituting Eq. (4.8c) into Eq. (4.8), we have

$$\nu(t,\theta) = c_L(t)\Delta x \cdot \frac{\Delta x}{2} k(0,\theta-t)\Delta\theta. \tag{4.9}$$

But, since we are in the diffusion limit of the random walk, we can take advantage of Eq. (4.1) and write the above formula as

$$\nu(t,\theta) = Dc_L(t)k(0,\theta-t)\Delta t\Delta\theta. \tag{4.10}$$

Integrating over all possible time subintervals likely to contribute, we deduce

$$\int_0^\theta \nu(t,\theta)dt = \Delta\theta\int_0^\theta Dc_L(t)k(0,\theta-t)dt. \tag{4.11}$$

Dividing by $\Delta\theta$, we get the contribution to the flux formula (2.14) from the left concentration. A similar derivation would also yield the contribution from the right end concentration.

The identification of Eq. (4.11), with the flux formula (2.14) and (2.24), provides a trajectory interpretation of the flux formula—particulary of the function $k(x,t) = q_x(x,t)$—and gives a computational, trajectory-based method to find the flux. The trajectories are just random walks as described in Sec. III, and the statistical measure of importance can, on the basis of Eq. (4.8b), be either $k(0,\theta-t)$ or $q(\Delta x/2,\theta-t)$. The latter is easier both to compute and to understand, and will form the basis for the calculations of Sec. VII.

A final remark: by definition, k is the x derivative of the probability function q. Hence, it can either be positive or negative. Therefore, even though k enters into the flux formula, k is not a probability density function. However, because of the absorbing boundary conditions, the positive function q essentially vanishes on both end boundaries and therefore

$$\begin{aligned} &q_x(0,t) = k(0,t) > 0, \\ &q_x(d,t) = k(d,t) < 0. \end{aligned} \tag{4.12}$$

In that sense, the quantities $k(0,t)$ and $-k(d,t)$ can be thought of as probability densities.

V. THE REDUCED LANGEVIN EQUATION

In this section, we relate the random walk formulation of Sec. III to the Langevin approach, based on a stochastic differential equation[25-27] widely used in the chemistry literature. This has twin advantages: it yields another computational method for arbitrary potentials and it ties us to the extensive chemistry literature on barrier crossing problems.

The simplest, and most traditional way, of describing the random walk introduced previously, is by means of the probability distribution $P_{n,m}$ of the particle being at $n\Delta x$ at time $t=m\Delta t$. By considering how a walker can reach location n at time step $m+1$, having started at time step m, we deduce the following difference equation for $P_{n,m}$:

$$P_{n,m+1} = P_{n+1,m}\cdot l_{n+1} + P_{n-1,m}\cdot r_{n-1} + P_{n,m}\cdot(1-r_n-l_n). \tag{5.1}$$

We complete the formulation of the problem for $P_{n,m}$, by specifying what happens when the particle reaches the extremities of the interval, as well as the initial starting point of the particle. In the diffusion limit, this formulation leads to the Smoluchowski equation

$$p_t = -(\mu p)_x + Dp_{xx}. \tag{5.2}$$

The above description is reminiscent of the Eulerian description used in fluid dynamics[28] which relies on observations about flow fields made with a fixed spatial coordinate system. Fluid dynamics also uses another description of flow, namely the Lagrangian description, in which the observer is, so to speak, riding with the fluid particle. The Lagrangian approach to the random walk yields the Langevin equation, as we shall see.

Let

$$X(j\Delta t) \equiv X_j \tag{5.3}$$

represent the location of the particle at the jth time step. Then

$$X_{j+1}=X_j+W_j\Delta x \tag{5.4}$$

represents the location of the particle at the next time step, where

$$W_j=\begin{cases}1 & \text{with probability } r_j\\ 0 & \text{with probability } 1-r_j-l_j\\ -1 & \text{with probability } l_j\end{cases} \tag{5.5}$$

Actually, it is preferable to split the motion into the drift and random parts. To that effect, we return to Eq. (3.10) and rewrite Eq. (5.4) as

$$X_{j+1}=X_j+\frac{(\Delta x)^2}{2D}\mu(X_j)+\tilde{R}_j\Delta x, \tag{5.6}$$

where

$$\tilde{R}_j=\begin{cases}1 & \text{with probability } s_j/2\\ 0 & \text{with probability } 1-s_j\\ -1 & \text{with probability } s_j/2\end{cases} \tag{5.7}$$

is a random variable. Since we shall continue to work in the diffusion limit, we can rewrite Eq. (5.6) as

$$X_{j+1}=X_j+\mu(X_j)\Delta t+\tilde{R}_j\Delta x. \tag{5.8}$$

Note that the mean value of the random variable $\tilde{R}_j$ is zero. We record this by writing

$$\langle\tilde{R}_j\rangle=0. \tag{5.9}$$

On the other hand, Eq. (5.7) implies that the mean square value of this random variable is

$$\langle\tilde{R}_j^2\rangle=s_j. \tag{5.10}$$

Since the random walk is a process in which each step is independent of the preceding one, we generalize this formula by writing

$$\langle\tilde{R}_j\tilde{R}_k\rangle=s_j\delta_{jk}. \tag{5.11}$$

The stochastic difference equation (5.8), with a random variable $\tilde{R}_j$ which satisfies the two properties (5.9) and (5.11), constitutes the "reduced" discrete Langevin equation.

We examine next, in a formal way, the diffusion limit of the above difference equation. First, we introduce another random variable

$$R_j=\tilde{R}_j\frac{\Delta x}{\Delta t}. \tag{5.12}$$

From Eqs. (5.9) and (5.11), we immediately deduce that

$$\begin{aligned}&\langle R_j\rangle=0,\\ &\langle R_jR_k\rangle=\frac{(\Delta x)^2}{(\Delta t)^2}s_j\delta_{jk}.\end{aligned} \tag{5.13}$$

We note in passing that

$$\sum_k\langle R_jR_k\rangle=\frac{(\Delta x)^2}{(\Delta t)^2}\sum_k s_j\delta_{jk}=\frac{(\Delta x)^2}{(\Delta t)^2}s_j$$

or better still

$$\sum_k\langle R_jR_k\rangle\Delta t=\frac{(\Delta x)^2}{\Delta t}s_j. \tag{5.14}$$

In the diffusion limit, the above expression becomes

$$\int_0^\infty\langle R(t)R(t')\rangle dt=2\cdot D\cdot 1=2D. \tag{5.15}$$

As a result, the reduced continuous Langevin equation is given by

$$\frac{dX(t)}{dt}=\mu[X(t)]+R(t), \tag{5.16}$$

where

$$\begin{aligned}&\langle R(t)\rangle=0,\\ &\langle R(t)R(t')\rangle=2D\delta(t-t').\end{aligned} \tag{5.17}$$

In closing this section, we state that no matter how weird an ordinary differential equation the reduced Langevin equation is, it provides a clear definition of a simulation. It certainly is easier to deal with numerically than the Smoluchowski equation (5.2), if only because the latter is a partial differential equation. Of course, an ordinary differential equation describing the steady state or mean flux would not be so hard to deal with as Eq. (5.2), nor so time consuming to compute as a Langevin simulation.

VI. THE FULL LANGEVIN EQUATION

The reduced Langevin equation (5.16) arises from a random walk, hopping-type model. The more commonly studied Langevin situation occurs when the Smoluchowski limit may not hold, and momentum must be considered.[29,30] Then the full Langevin equation is

$$\begin{aligned}&\frac{dX}{dt}=V(t),\\ &\frac{dV}{dt}=\beta\{-V+\mu[X(t)]+R(t)\},\end{aligned} \tag{6.1}$$

where

$$\beta=\frac{kT}{mD} \tag{6.2}$$

m being the mass of the particle undergoing the random walk. The time necessary for the particle to acquire a Maxwellian velocity distribution, namely, the so-called "relaxation time" of velocity, is of $O(\beta^{-1})$. When the relaxation time is short compared to the evolution time, say $d(m/E)^{1/2}$, where E is a barrier height, that is to say, when

$$\begin{aligned}&\epsilon\equiv\frac{\beta^{-1}}{d(m/E)^{1/2}}\ll 1,\\ &\epsilon\equiv\frac{D(mE)^{1/2}}{dkT}\ll 1,\end{aligned} \tag{6.3}$$

then for $t\beta \gg 1$ the trajectory of the particle can be obtained via the reduced Langevin equation, though this is difficult to prove mathematically.[31]

Without attempting to prove this statement, we can make it plausible by proceeding formally with the beginning of a two-time asymptotic analysis of the problem.[32] Glossing over the details, we consider the limiting process, t fixed $\beta \to \infty$ and look for a solution of the form

$$X(t;\beta) = X^{(0)}(t) + \tfrac{1}{\beta} X^{(1)}(t) + \cdots,$$
$$V(t;\beta) = V^{(0)}(t) + \tfrac{1}{\beta} V^{(1)}(t) + \cdots. \tag{6.4}$$

Substituting the representations (6.4) into the Langevin equation (6.1), we deduce that, to zeroth order

$$\frac{dX^{(0)}}{dt} = V^{(0)}(t),$$
$$0 = -V^{(0)} + \mu[X^{(0)}(t)] + R(t), \tag{6.5}$$

or equivalently

$$\frac{dX^{(0)}}{dt} = \mu[X^{(0)}(t)] + R(t), \tag{6.6}$$

which is the reduced equation (5.16) previously deduced from the random walk.

We have thus connected the Smoluchowski equation (5.2) first to the reduced Langevin equation, and then to the full Langevin equation in order to extend the validity of our flux formula. Strictly speaking, this extension is only valid for the case $\epsilon \ll 1$. A more rigorous approach would require us to start from the full Fokker–Planck equation[33] with concentration boundary conditions, and then derive a more general flux formula via the appropriate adjoint problem. This adjoint problem, viewed as an Eulerian description of a stochastic process would then be phrased in terms of a Lagrangian description, which hopefully would be identical to the full Langevin equation.

The full Langevin equation of Eq. (6.1) is, of course, an inadequate representation of the full dynamics of ion motion. For barrier crossings, both in ion channels and in chemical reactions, generalized Langevin equations, with a nonlocal friction kernel, are used to deal both with the inertial behavior at short times, and with the coupled-mode behavior at longer times.[7–9,10,11,34,35] Though a generalization of the techniques used here might well be employed in conjunction with a generalized Langevin description, that is really quite aside from the focus of our work, which is the proper formulation of the barrier crossing problem with concentration boundary conditions.

VII. COMPUTATION OF FLUX FROM PARTICLE TRAJECTORIES

The aim of our work is to develop appropriate particle trajectory methods to calculate the steady state flux of ions at the right-hand boundary subject to the concentration boundary conditions. To do so, we have first derived the steady state flux formula (2.24) in terms of $\mathcal{K}_0(0)$ and $\mathcal{K}_0(d)$. To obtain the flux by a trajectory method we shall rely on the stochastic interpretation of these quantities for their computation. Such an interpretation was given in Sec. IV, where we showed that $\mathcal{K}_0(0)$ is the limit, as $\Delta x \to 0$, of the probability of a particle which starts at Δx to be absorbed at the right end. We shall therefore release particles very near the left boundary, follow their evolution via one of the three schemes, viz., the discrete random walk of Eq. (5.8), the reduced (continuous) Langevin equation of Eq. (5.16), or the ordinary Langevin equation of Eq. (6.1), and keep track of whether these particles reach the right boundary, and, if so, record the elapsed times. Of course, we can also evaluate $\mathcal{K}_0(d)$ and $\mathcal{K}_0(0)$ exactly for any given potential and we shall do so to check the accuracy of our trajectory methods.

To track particle trajectories, we discretize space and time and introduce the integers M,N once again. Recall that

$$(N+1)\Delta x = d,$$
$$(M+1)\Delta t = \theta. \tag{7.1}$$

With this discretization

$$\mathcal{K}_0(0) = \int_0^\theta k(0,t)\,dt \approx \sum_{j=1}^{M+1} k(0,j\Delta t)\Delta t$$
$$\approx \sum_{i=0}^{M} K_{1/2,i}$$
$$= \frac{1}{\Delta x} \sum_{i=0}^{M} (Q_{1,i} - Q_{0,i})$$
$$= \frac{1}{\Delta x} \sum_{i=0}^{M} Q_{1,i}. \tag{7.2}$$

The three last equations follow, respectively, from Eqs. (4.4), (3.9a), and (3.13). Now $Q_{1,i}$, from Sec. III, is the probability that a particle starting from Δx reaches d for the first time in the interval $[(i-1)\Delta t, i\Delta t]$. Then, clearly, $\Sigma_{i=0}^{M} Q_{1,i}$ is the cumulative probability that a particle starting its walk at Δx reaches d in the time interval $(0,\theta)$.

We now define N_s^0 as the number of successful trajectories, obtained by simulation from random walk, reduced Langevin or Langevin propagation. Similarly, N_f^0 is the number of unsuccessful walks (absorbed at $x=0$) starting from that same point. Then clearly

$$\sum_{i=0}^{M} Q_{1,i} = \frac{N_s^0}{N_s^0 + N_f^0}. \tag{7.3}$$

These same arguments can be applied to the second term in Eq. (2.24). We have

$$\mathscr{K}_0(d) \approx \int_0^\theta k(d,t)dt \approx \sum_{j=1}^{M+1} k[(N+1)\Delta x, j\Delta t]\Delta t$$
$$\approx \sum_{i=0}^{M} K_{N+1/2,i}$$
$$= \frac{1}{\Delta x}\sum_{i=0}^{M}(Q_{N+1,i}-Q_{N,i})$$
$$= \frac{1}{\Delta x}\left[1-\sum_{i=0}^{M} Q_{N,i}\right]$$
$$= \frac{1}{\Delta x}\left[1-\frac{N_s^d}{N_s^d+N_f^d}\right]. \tag{7.4}$$

Here we have defined N_s^d as the number of trajectories that start from $(d-\Delta x)$ and reach d in the interval $(0,\theta)$. Similarly, N_f^d is the number of trajectories that start at $(d-\Delta x)$ and disappear at $x=0$. Incidentally, the time θ in these simulations must be long enough that essentially all the random walkers suffer one of these fates; no one is still walking on the lattice at $t=\theta$.

Then the solution for the steady-state flux is just

$$J=\frac{1}{\Delta x}\left[-Dc_R\left(\frac{N_f^d}{N_s^d+N_f^d}\right)+Dc_L\left(\frac{N_s^0}{N_s^0+N_f^0}\right)\right]. \tag{7.5}$$

This is the simulation version of the steady-state flux formula (2.24)

The flux is obtained by starting *independent* particles from position Δx and following them by one of the three schemes, viz. Eq. (5.8), (5.16), or (6.1). By running many successive random trajectories, we evaluate the numbers N_s^0 and N_f^0, simply by counting how many of these trajectories end on the right or left side. Similarly, we follow a number of trajectories starting at $x=d-\Delta x$, and thus evaluate N_s^d and N_f^d. From the values of c_R, c_L, N_s^0, N_f^0, N_s^d, N_f^d, D, and Δx, we find the flux from Eq. (7.5).

VIII. ACTIVATION BEHAVIOR: THE HIGH BARRIER CASE

The formulation given thus far is entirely general, and derives the continuum flux subject to concentration boundary conditions. To make contact with standard chemical rate formulations, we will consider the case of a steady-state flow, when a single high barrier is found along the x coordinate, which corresponds to the channel length in the ion transport case, and, more generally, to the reaction coordinate in bimolecular reactions.

We start by rewriting the flux formula (2.24), in which $\mathscr{K}_0(0)$ and $\mathscr{K}_0(d)$ are replaced by their explicit forms as given by Eq. (2.25), namely,

$$J=D\frac{c_L\exp[(Ze/kT)\phi(0)]-c_R\exp[(Ze/kT)\phi(d)]}{\int_0^d \exp[(Ze/kT)\phi(\xi)]d\xi}. \tag{8.1}$$

We next evaluate the integral entering into this expression approximately. Just as in the classical Kramers analysis,[36] we suppose now that the potential ϕ has a high, narrow peak at the position $x=h$, far from the boundary. In particular, we assume that

$$\frac{Ze}{kT}\phi(h)\gg 1, \tag{8.2}$$

$$\phi(h)\gg\phi(d),\quad \phi(0). \tag{8.3}$$

Assuming furthermore that the potential is smooth, we write

$$\phi(x)=\phi(h)+\tfrac{1}{2}\phi''(h)(x-h)^2+\cdots. \tag{8.4}$$

Substituting this parabolic approximation of ϕ in the integral, we write

$$\int_0^d \exp\left[\frac{Ze}{kT}\phi(\xi)\right]d\xi$$
$$\approx \int_{-\infty}^{\infty} d\xi \exp\left[\frac{Ze}{kT}\phi(h)\right]$$
$$\times\exp\left[-\frac{e}{2kT}(\xi-h)^2|Z\phi''(h)|\right]$$
$$=\exp\left[\frac{Ze}{kT}\phi(h)\right]\sqrt{\frac{2\pi kT}{e|Z\phi''(h)|}}. \tag{8.5}$$

As a result

$$J\approx D\left[c_L\exp\left[\frac{Ze}{kT}\phi(0)\right]-c_R\exp\left[\frac{Ze}{kT}\phi(d)\right]\right]\sqrt{\frac{e|Z\phi''(h)|}{2\pi kT}}\exp\left[-\frac{Ze}{kT}\phi(h)\right]. \tag{8.6}$$

Equation (8.6) is highly reminiscent of activated complex theory, and the Kramers[36] formulation of bimolecular rate theory. Rewritten, it states that the rate constant, defined as the flux divided by the diffusion coefficient times the concentration gradient, is equal to a prefactor times the exponential of an activation energy. The prefactor is simply proportional to the frequency (square root of curvature of the potential) at the barrier top.

We may interpret Eq. (8.6) in terms, as usual, of a quasiequilibrium at steady state between a small number of "particles" at the barrier peak and the concentration in the right and left boundaries. If the simulation were begun either from the left or the right, very few of the simulation particles would reach the barrier top. As in Kramers' theory, the flux depends sensitively on the local features of the potential at the barrier top. It is worth noting that the results of Eq. (8.6) are derived solely from a continuum picture in steady state. It does not make the specific assumption of pre-equilibrium between activated complex and reactant, which is usually stated as the basis of activated complex rate theory.

The expression for the concentration at the top of the barrier, mentioned above, can be written as part of the same approximation

$$c(h)=\exp\left[-\frac{Ze}{kT}\phi(h)\right]\frac{c_L\exp[(Ze/kT)\phi(0)]+c_R\exp[(Ze/kT)\phi(d)]}{2}. \tag{8.7}$$

This important, intuitively reasonable result says that the concentration at the barrier height depends only on the Boltzmann factor at the barrier height, and on the average concentrations on the right and the left of the barrier.

In addition to providing a link with standard chemical rate processes,[7-9,34,35,37-42] Eq. (8.6) helps to interpret the numerical simulations of ion flow in the case of a potential barrier; the population factor $\exp[-Ze\phi(h)/kT]$ is a measure of the likelihood of the particle climbing over the potential, and should be compared with the results of simulations. This comparison, and a general simulation for particular barrier shapes, can now be presented.

IX. EXAMPLES: DIFFUSION OVER ECKART BARRIERS

The formulation of the barrier-crossing flux problem that is presented in Secs. II–VII holds for arbitrary one-dimensional potentials $\phi(x)$, subject to concentration boundary conditions. In Sec. VIII, the special case of a single dominant peak in the barrier, of potential energy well in excess of kT, is presented. The steady-state flux can be computed from Eq. (7.5) in five different ways: by means of the the exact formula (8.1), by the approximation for high barriers as given analytically by (8.6), and by three possible schemes for simulation (Langevin dynamics, reduced Langevin dynamics and random walk), all of which can be used to calculate the numbers of successful and unsuccessful trajectories from the right and left sides of the barrier. In this section we present numerical results for typical potentials, showing how well the trajectory methods and high-barrier approximation reproduce the exact results.

For computational purposes, we write the reduced Langevin equation (5.16) as

$$\Delta X=\mu[X(t)]+\sqrt{2D}\xi(\Delta t)^{1/2}, \tag{9.1}$$

where ξ is a random variable with a distribution $f(\xi)$ such that

$$\int_{-\infty}^{\infty}\xi f(\xi)d\xi=0,\qquad \int_{-\infty}^{\infty}\xi^2 f(\xi)d\xi=1. \tag{9.2}$$

We have used various forms of f in our calculations. In particular, we have used

(a) the lattice distribution

$$f_1(\xi)=\begin{cases}1/2 & \text{for } \xi=1\\ 1/2 & \text{for } \xi=-1\\ 0 & \text{otherwise;}\end{cases} \tag{9.3}$$

(b) the Gaussian distribution

$$f_2(\xi)=\frac{1}{\sqrt{2\pi}}\exp\left(-\frac{\xi^2}{2}\right); \tag{9.4}$$

(c) the uniform random distribution between finite limits

$$f_3(\xi)=\begin{cases}1/(2\sqrt{3}) & \text{for } -\sqrt{3}\leqslant\xi\leqslant\sqrt{3}\\ 0 & \text{otherwise;}\end{cases} \tag{9.5}$$

(d) the two-Gaussian distribution

$$f_4(\xi)=\frac{1}{2\sqrt{\pi}}\{\exp[-(\xi-1)^2]+\exp[-(\xi+1)^2]\}. \tag{9.6}$$

The potential barriers used in this paper are of the Eckart form[43] often used to describe energy profiles in chemical reactions. While the energy (or free energy) barrier for ion passage through biological channels is less well characterized, the Eckart profiles of Fig. 2 are intuitively reasonable for ion flow, and similar forms are often used in the channel problem. The difference in potential between $x=0$ and $x=100$ Å is the transmembrane potential measured or controlled in physiological experiments.

Figure 2 shows the different Eckart potentials with different barrier heights, namely, small, medium, large, and largest. Figure 2(a) shows barriers that are small, less than kT, for forward movement. Figure 2(c) shows a barrier small for forward movement and reasonably large for backward movement. Figure 2(d) shows a barrier that is high for both the forward and backward movements.

Distance is specified in the Eckart potentials by the reduced distance variable ξ

$$-\xi\equiv\exp\left(\frac{2\pi x}{L}\right). \tag{9.7}$$

The potential functions are then

$$Ze\phi=-\frac{A\xi}{1-\xi}-\frac{B\xi}{(1-\xi)^2}, \tag{9.8}$$

with L a typical barrier width, corresponding say to a channel width d. The parameter A gives the exoergicity (potential energy difference) for the barrier crossing, with the barrier height from the left being $(A+B)^2/4B$.

Integrals of exponentials occur widely in our analysis and have a simple dependence on the length d of the channel, if the potential depends only on x/d, as do the Eckart potentials, where $\phi(x)=\Phi(y)$, with $y=x/d$

$$\int_0^d\exp\left[\frac{Ze\phi(x)}{kT}\right]dx=d\int_0^1\exp\left[\frac{Ze\Phi(y)}{kT}\right]dy\propto d. \tag{9.9}$$

Thus trajectories are computed in a shortened channel, namely from 0 to $\delta<d$, taking less computer time than computations reaching from 0 all the way to d. Estimates of the truncated integrals, computed from 0 to δ, are then multiplied by d/δ to estimate the original integrals, extend-

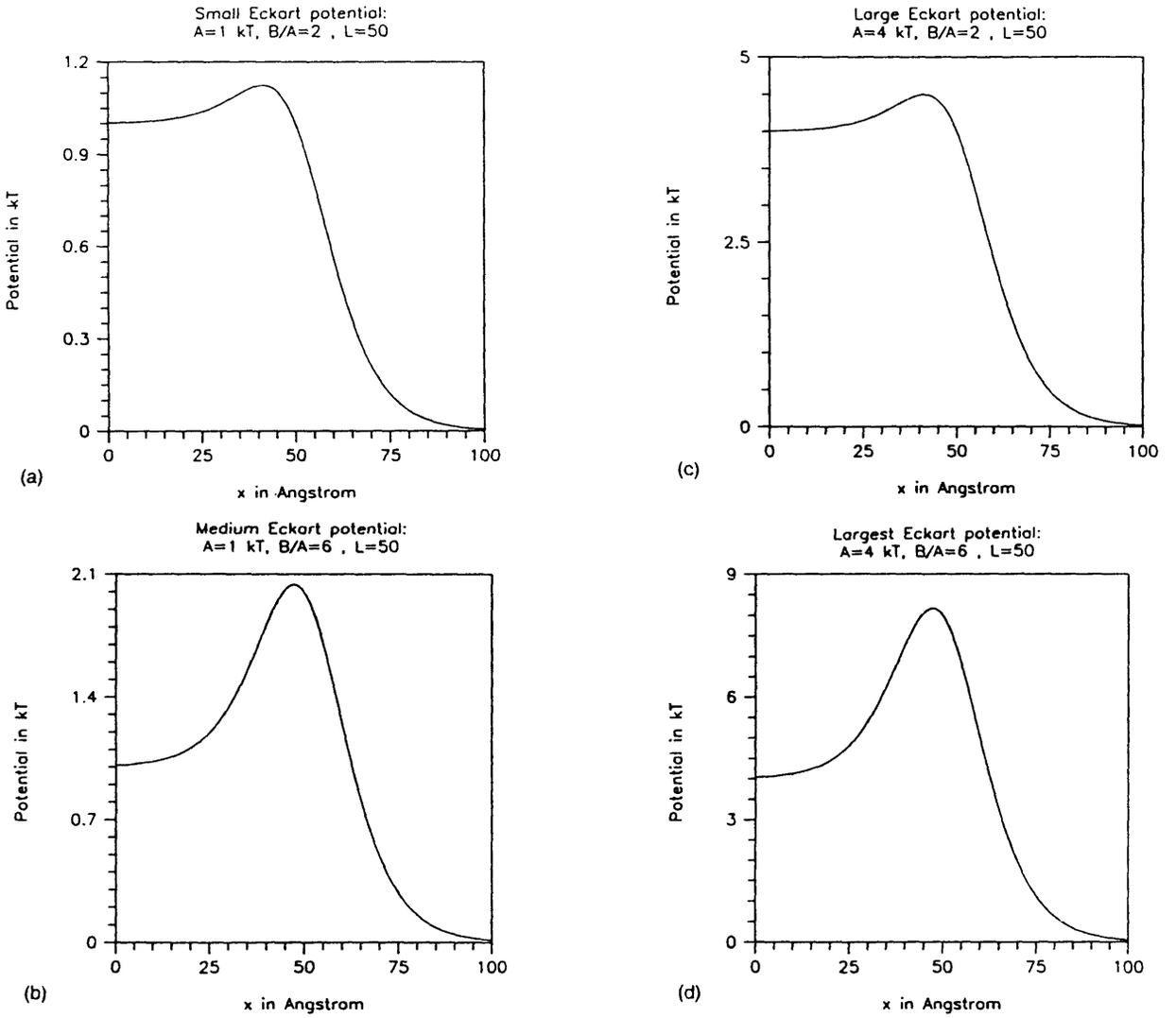

FIG. 2. Asymmetrical Eckart potentials. Variations on the parameters A and B produce four different characteristic shapes, with barrier heights smaller than, comparable to, or larger than kT.

ing from 0 to d; of course, the shorter distance δ must remain large compared to the discretization Δx used in computing the trajectories.

We turn now to the numerical estimates of both the forward and backward flux. These were made using all five methods and are presented in Tables I and II. The accompanying figures show corresponding trajectories, in both directions, usually with different time scales on the top and bottom horizontal scales. Histograms are also shown of the first-passage times from left to right $Q(\Delta x,t)$ or from right to left $Q(d-\Delta xt)$; see Eqs. (3.3), (4.8c), (7.2), (7.4), and captions for precise definitions. Calculations were performed with parameters that might describe biological channels, namely,

$D=1.0\times10^{-5}$ cm^2/s;

$d=100$ Å;

$m=23$ Dalton;

$T=298$ °K.

Table III suggests that biological channels are in the high friction domain, heavily damped, allowing use of the reduced Langevin equation: the dimensionless ratio ϵ of Eq. (6.3), i.e., the ratio of the relaxation time of velocity to the characteristic evolution time, is less than 0.01 for all four Eckart barriers considered here.

Several conclusions follow from these data:

(1) The random walk, Langevin, and reduced Langevin methods give essentially identical results for this set of model potentials. For less strongly damped situations (i.e., larger ϵ), the reduced Langevin and random walk representations will be inadequate, as has been suggested for one biological channel.[44]

(2) Estimates made from simulations of trajectories are quite close to the exact results, for both forward and backward fluxes, with errors less that 10% in all cases. For small barriers, numerical estimates are less subject to errors because the sums in Eq. (7.5) converge more quickly; the errors are then negligible. Thus calculations of trajectories are an accurate way to determine fluxes, although they are more sparing of intellectual than computer resources.

(3) The effective velocity of ion movement through channels is quite small compared to thermal velocities,

TABLE I. The calculation of flux over the Eckart potential by *random walk* scheme. Note: Δx is the distance away from the absorbing boundaries at which the trajectories start. The errors in the $\mathcal{K}_0$'s are the normalized standard deviations of the estimate of $\mathcal{K}_0$'s. The $\mathcal{K}_{\text{exact}}$ is given by $\mathcal{K}_0(x)_{\text{exact}}=\exp[e\phi(x)/kT]/\int_0^d \exp[e\phi(\xi)/kT]d\xi$ and is evaluated numerically by the Gauss–Kronrod method. Other parameters are $d=100$ Å, $m=23$ amu, $D=1.0\times10^{-5}$ cm^2/s. The $\mathcal{K}_{\text{sim}}$ are defined as follows: $\mathcal{K}_0(0)_{\text{sim}}=(1/\Delta x)\ [N_s^0/(N_s^0+N_f^0)]$; $\mathcal{K}_0(d)_{\text{sim}}=(1/\Delta x)\ [N_f^d/(N_s^d+N_f^d)]$.

Eckart parameters	Small barrier $A=1$, $B/A=2$	Medium barrier $A=1$, $B/A=6$	Large barrier $A=4$, $B/A=2$	Largest barrier $A=4$, $B/A=6$
$\mathcal{K}_0(0)_{\text{exact}}$	1.288×10^{-2}	8.464×10^{-3}	1.476×10^{-2}	1.156×10^{-3}
$\mathcal{K}_0(0)_{\text{sim}}$	1.285×10^{-2}	8.557×10^{-3}	1.496×10^{-2}	1.262×10^{-3}
Error in $\mathcal{K}_0(0)$	2%	5%	2%	2%
$\mathcal{K}_0(d)_{\text{exact}}$	4.753×10^{-3}	3.125×10^{-3}	2.744×10^{-4}	2.150×10^{-5}
$\mathcal{K}_0(d)_{\text{sim}}$	4.759×10^{-3}	3.118×10^{-3}	2.780×10^{-4}	1.997×10^{-5}
Error in $\mathcal{K}_0(d)$	1%	0.5%	2%	2%
N_s^0	5 000	5 000	5 000	5 000
N_f^0	3 835 342	5 837 728	3 373 950	40 463 540
N_s^d	10 511 633	15 982 700	17 561 150	997 910 170
N_f^d	5 000	5 000	5 000	2 000
Δx (Å)	0.1	0.1	0.1	0.1

even for relatively small barriers, if we define effective velocity as flux divided by concentration. Therefore, even small barriers in channels will serve to impede ion flow substantially compared to free diffusion; evolutionarily, this can lead to selectivity if potential barriers differ slightly for different ions because, for example, different ions (and their adjoining waters) fit slightly differently into the potential wells of the biological[45] or crystalline[46] channel.

(4) Table IV shows that the high barrier approximate expression is in error by at least 15% for all eight of the computed fluxes even though a number of these fluxes cross quite high barriers. Figure 3 shows why: The approximation assumes a symmetrical quadratic form of the potential, while our Eckart potentials are quite asymmetrical. (Needless to say, the approximation is best when the barrier is highest, other things being equal.) Interestingly, the error appears in the prefactor, not the barrier height, when the fluxes or rates are written in Arrhenius form (8.6).

(5) The histograms $Q_{1,i}$, $Q_{N,i}$, displayed in Fig. 4, summarize the simulations and estimate the likelihood that particles starting at $x=\Delta x$ or $x=d-\Delta x$, respectively, reach the opposite boundary after i time intervals. These histograms all have roughly the same form: At very short times, $Q_{1,i}$ and $Q_{N,i}$ both vanish, because the particles have not had sufficient time to cross the barrier in either direction. As time increases, the value of these Q's grows until they reach a maximal value, the most probable time for crossing the channel. The values shown here are reasonable estimates for the first-passage time of an ion crossing a biological channel.[47–49] For longer times, the Q's fall off slowly because the probability for the particle of surviving in the channel decreases monotonically with time. As pointed out in Sec. VII, the duration of our simulations must be long enough to allow all particles to exit the channel. The required time is clearly much larger for high barriers than for low ones.

(6) The values for the current through the open chan-

TABLE II. The calculation of flux over the Eckart potential by *reduced Langevin* scheme. Note: Δx is the distance away from the absorbing boundaries at which the trajectories start; Δt is the time step. The errors in the $\mathcal{K}_0$'s are the normalized standard deviations of the estimate of $\mathcal{K}_0$'s. The $\mathcal{K}_{\text{exact}}$ is given by $\mathcal{K}_0(x)_{\text{exact}}=\exp[e\phi(x)/kT]/\int_0^d \exp[e\phi(\xi)/kT]d\xi$ and is evaluated numerically by the Gauss–Kronrod method. Other parameters are $d=100$ Å, $m=23$ amu, $D=1.0\times10^{-5}$ cm^2/s. The $\mathcal{K}_{\text{sim}}$ are defined by $\mathcal{K}_0(0)_{\text{sim}}=(1/\Delta x)\ [N_s^0/(N_s^0+N_f^0)]$; $\mathcal{K}_0(d)_{\text{sim}}=(1/\Delta x)\ [N_f^d/(N_s^d+N_f^d)]$.

Eckart parameters	Small barrier $A=1$, $B/A=2$	Medium barrier $A=1$, $B/A=6$	Large barrier $A=4$, $B/A=2$	Largest barrier $A=4$, $B/A=6$
$\mathcal{K}_0(0)_{\text{exact}}$	1.288×10^{-2}	8.464×10^{-3}	1.476×10^{-2}	1.156×10^{-3}
$\mathcal{K}_0(0)_{\text{sim}}$	1.284×10^{-2}	8.410×10^{-3}	1.477×10^{-2}	1.175×10^{-3}
Error in $\mathcal{K}_0(0)$	5%	5%	1%	2%
$\mathcal{K}_0(d)_{\text{exact}}$	4.753×10^{-3}	3.125×10^{-3}	2.744×10^{-4}	2.150×10^{-5}
$\mathcal{K}_0(d)_{\text{sim}}$	4.915×10^{-3}	3.225×10^{-3}	2.976×10^{-4}	2.061×10^{-5}
Error in $\mathcal{K}_0(d)$	4%	2%	3%	4%
N_s^0	5 000	5 000	5 000	5 000
N_f^0	777 300	1 184 210	668 310	8 488 590
N_s^d	2 026 900	3 109 550	33 584 260	498 952 585
N_f^d	5 000	5 000	5 000	5 000
Δx (Å)	0.5	0.5	0.5	0.5
Δt (pS)	5.0×10^{-4}	5.0×10^{-4}	5.0×10^{-4}	5.0×10^{-4}

TABLE III. The validity of the Smoluchowski limit. Note: ϵ is defined by Eq. (6.3), where E is the value of the barrier height and T is room temperature.

Eckart parameters	Small barrier $A=1$, $B/A=2$	Medium barrier $A=1$, $B/A=6$	Large barrier $A=4$, $B/A=2$	Largest barrier $A=4$, $B/A=6$
ϵ	2.005×10^{-3}	2.701×10^{-3}	4.009×10^{-3}	5.401×10^{-3}

nel in our calculations are given in Table V. These currents, roughly 1 pA, are physiologically very reasonable, particularly given our generous estimate of the length of the channel. Constant field theory is a traditional description of open channels,[3] recently derived in a fairly general way for certain special cases.[1]

(7) The behavior of some typical trajectories [as computed from Eq. (3.3)] is shown in Fig. 5. Note that the two different trajectories in each panel are usually shown at different time scales, one defined on the upper abcissa and the other on the lower. For both forward and backward crossing, the most probable trajectories are those that start and end on the same side of the barrier: these are the solid lines in Fig. 5. The time for barrier crossing (dotted trajectories) is *always* larger than for barrier reflection (solid trajectories); the latter trajectories are more probable because more random walkers are reflected by the barrier than pass over it. Barrier recrossing[35,40] is quite common—especially for low, flat barriers—as is clear from the dotted trajectories in Figs. 5(a1), 5(a2), and 5(b2). An incomplete search showed no cases in which a particle recrossed a high barrier after passing the maximum of the potential.

(8) The numbers N_s^d, N_f^d, N_s^0, and N_f^0 shown in Table I, clearly reflect comments (6) and (7) above. For high barriers, the rate constants and probabilities for passage over the barrier are small, as shown by the ratios N_s^0/N_f^0 and N_s^d/N_f^d. Note that the latter ratio, characterizing the reverse motion, is always smaller than the former, characterizing the forward motion, as would be expected for the asymmetric Eckart barriers of Fig. 2.

(9) When the particle starts close to the boundary, the Gaussian distribution had to be handled with care, since many of the displacements ξ moved the particle beyond (i.e., to the left of) the boundary at $x=0$. Two strategies were used. First, the particle was started far enough away from the boundary that it had only a small probability of moving beyond the boundary at $x=0$ in the first time step. Second, if the particle were started at $x=\Delta x$, a correction for the number of particles found between $-\infty$ and 0 was computed from the the analytical form of the Gaussian. There were no appreciable differences in the numerical results among these methods or the distributions (9.3)–(9.6), although there were substantial differences in how long they took to compute.

TABLE IV. The comparison of the high barrier approximation formula with the exact numerical integration. Note: λ is defined by $\lambda=\int_0^d \exp[e\phi(x)/kT]dx$. The subscripts exact and approx refer to the direct numerical integration and the high barrier approximation formula respectively. The error is defined by $\text{Error}=|\lambda_{\text{approx}}-\lambda_{\text{exact}}|/\lambda_{\text{exact}}$.

Eckart Parameters	Small barrier $A=1$, $B/A=2$	Medium barrier $A=1$, $B/A=6$	Large barrier $A=4$, $B/A=2$	Largest barrier $A=4$, $B/A=6$
λ_{exact}	2.116×10^{2}	3.242×10^{2}	3.726×10^{3}	4.901×10^{4}
λ_{approx}	1.638×10^{2}	1.825×10^{2}	2.394×10^{3}	4.171×10^{4}
Error	23%	44%	36%	15%

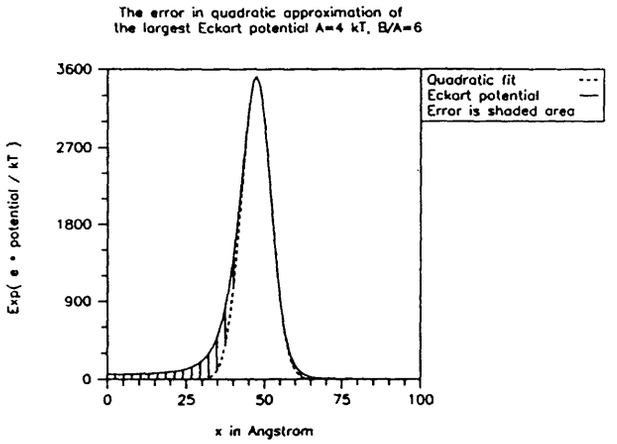

FIG. 3. The error involved in approximating the Eckart barrier by a quadratic approximation. The shaded area shows the difference between the exponential of the true potential and the exponential of the quadratic approximation. For asymmetric potentials, such areas are present, *no matter how large the barrier.*

The calculations were performed with an IBM RS/6000 Model 550 computer. The exact evaluation of the flux took only 2.0×10^{-3} s, whereas simulation of the flux with the reduced and full Langevin simulations required 30 h of CPU time for the low barrier and 180 h for the high barrier, when they were started at $x=3\Delta x$ or $x=d-3\Delta x$. Simulations of the flux as a random walk on the lattice, starting at $x=\Delta x$, took a factor of 10 less time to compute.

X. COMMENTS

Our interest in biological problems *forced* us to analyze barrier crossing in channels *as an explicit boundary value problem.* In the Kramers formulation[7,9,36,41] of the chemical reaction problem, the differential equation is accompanied (and the solution made unique) by physical statements, rather than by explicit boundary conditions. In particular, the equilibrium concentration of reactant is specified in a well of potential and particles are required to disappear once they cross the top of the potential barrier. Despite these differences, the boundary value and Kramers treatments give similar results, when barriers are high:[50] the flux is proportional to the diffusion constant and is of Arrhenius form (8.6).

Important generalizations of the Kramers analysis occur in the chemical literature involving such issues as multidimensionality;[35,51,52] frequency-dependent friction;[11,53,54] constrained or anisotropic diffusion;[35,55–57] and dielectric and mechanical contributions to the friction.[11] Experimen-

tal tests and applications of the Kramers' results and their generalizations have appeared,[8,58] and the case of intermediate friction, which Kramers[36] did not treat, has been analyzed.[9,13,42,59]

Most of these contributions have considered the standard problem of escape over a *single high* barrier. Some analysis has been made of more general barrier shapes, particularly those with several intervening minima,[60] such as would occur in a chain of reactions like $A \rightleftharpoons B \rightleftharpoons C$ that proceed through an intermediate or with essentially no barrier, as are appropriate for photoisomerization reactions.[61,62] Concentration boundary conditions on $[A]$, $[B]$, and $[C]$ might then be appropriate. The analysis given here treats this problem directly, since the overall flux formula (2.14) and its steady-state limit (2.24) hold for arbitrary potentials $\phi(x)$; indeed, the reactants can be specified anywhere along the potential, *not* just at minima. Thus both the analytic and trajectory counting methods given here can be used to analyze flux through intermediate states, as long as the concentration boundary conditions are appropriate.

Concentration boundary conditions have been finessed in the literature of biological channel crossing. In channel literature using activated complex theory, boundary conditions of any type rarely appear;[3] however, the analysis and justification in the chemical literature[7,9] applies quite directly to the channel situation. In diffusion based theories of channels, different boundary conditions have been proposed—after a combination of physical, probabilistic, and mathematical arguments—to describe the same physical situation, a channel connecting two solutions of known, and constant, concentration.[2,47,48,55,63–65] The present analysis uses only mathematics (with no additional physical argument or assumption) to analyze the consequences of these concentration boundary conditions, but it only treats the high friction limit. We derive a flux formula, (2.14) or (7.5), in terms of a specific stochastic problem (2.12) or (4.6) and show that the steady-state flux is a simple function (2.24) of moments—Eqs. (2.25), (2.18), (7.2), and (7.4)—of the stochastic problem. The stochastic problem can be solved analytically or by simulation of its trajectories, with indistinguishable results (Tables I, II,

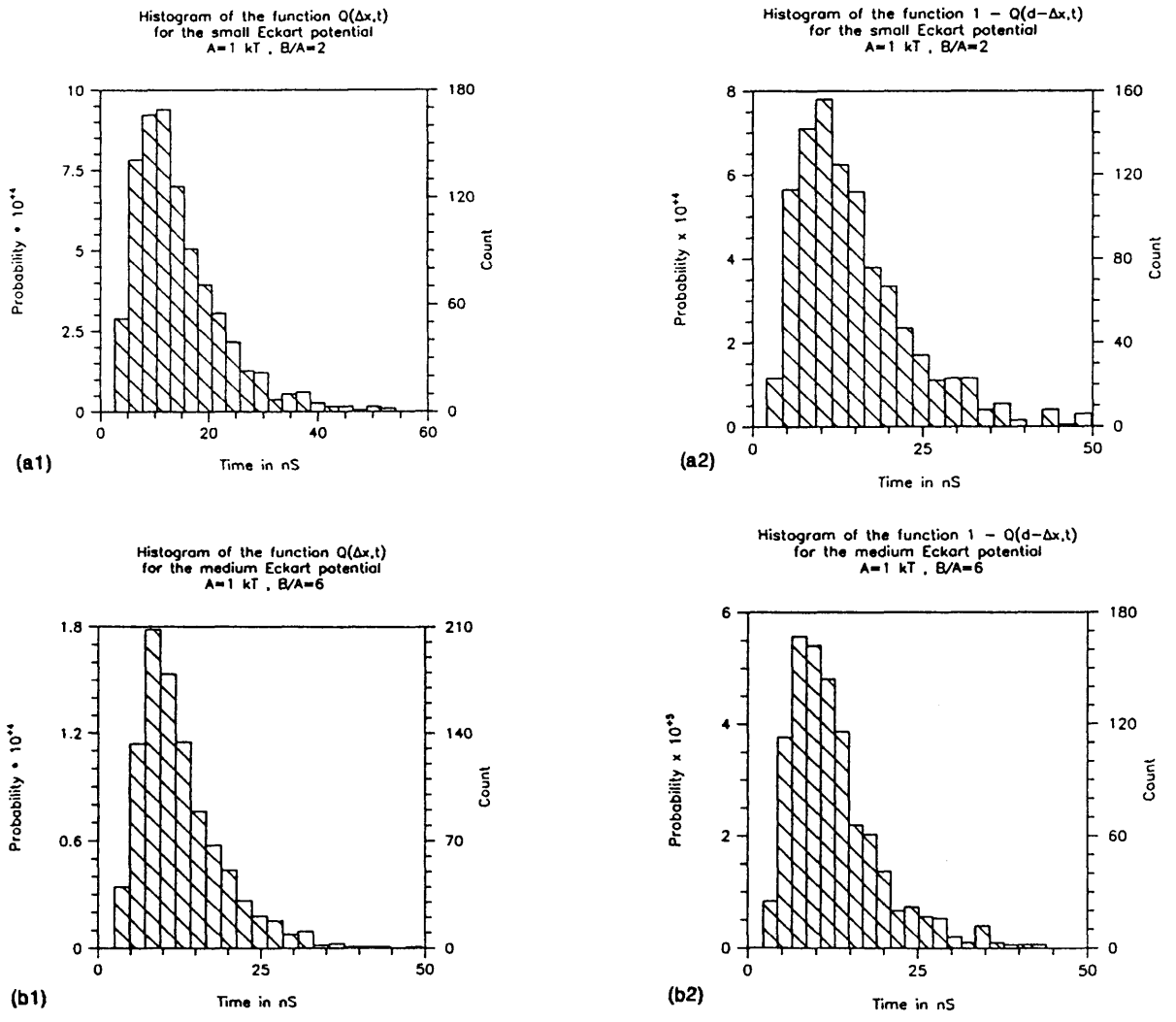

FIG. 4. Histograms of the function $Q(\Delta x,t)$, that determines the flux as described by Eqs. (7.2), (7.4), and (2.24). (a1), (b1), (c1), and (d1) show histograms of the forward trajectories and (a2), (b2), (c2), and (d2) show histograms of the backward trajectories.

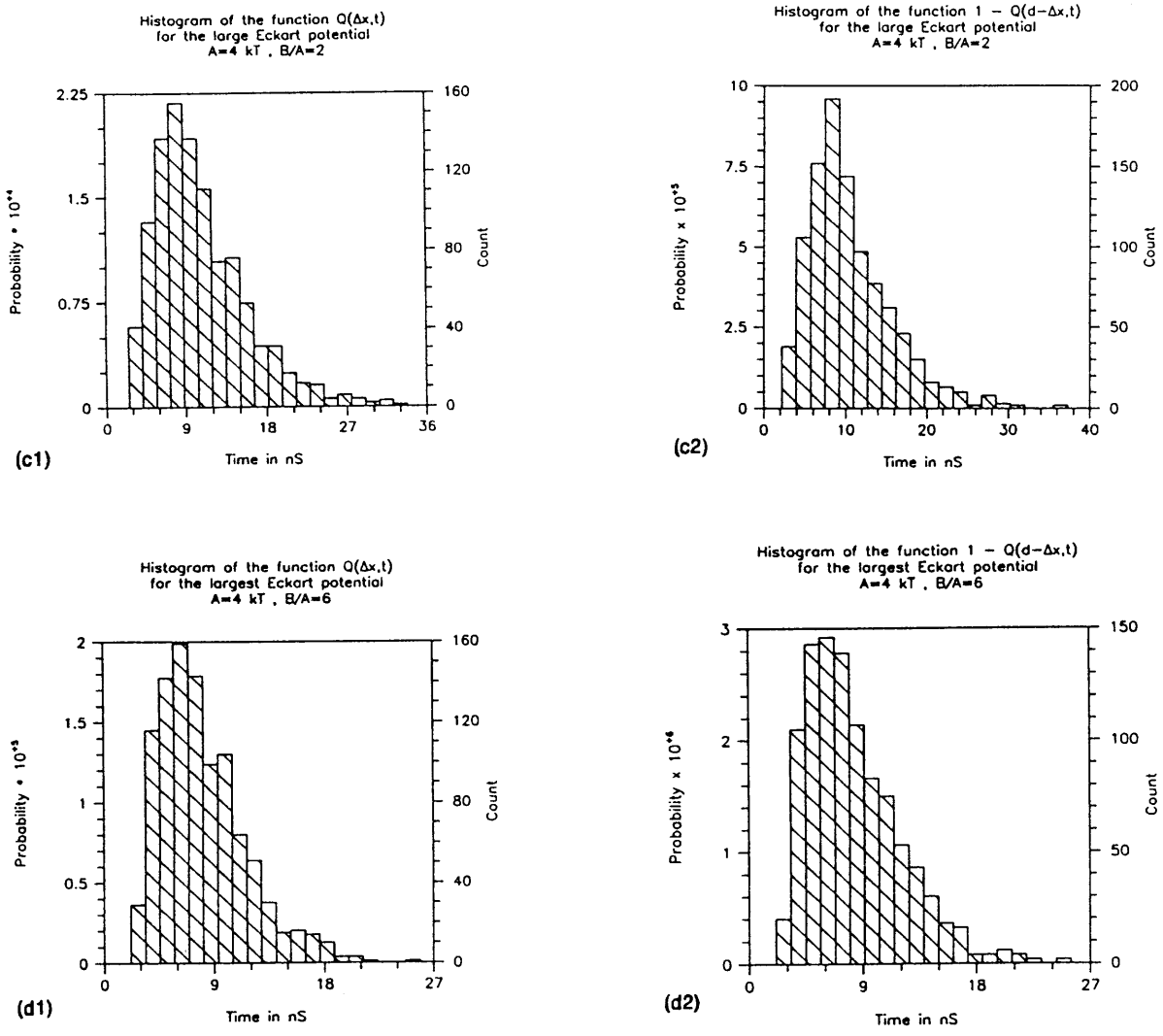

FIG. 4. (*Continued.*)

and VI), but those results appear to differ from previous results in the channel literature.

XI. CONCLUSIONS

The results presented here are perhaps most useful when applied to problems without analytical solutions, or in which Nernst–Planck equations are difficult to derive. If particles interact, it is easy to write, and not too hard to compute, Langevin equations, as has been done extensively in the literature of crystalline channels[46,66,67] in solid electrolytes. A generalization of the methods described here, particularly Eq. (2.14), may be useful in these cases, even if the associated Fokker–Nernst–Planck equations are not well known.

In actual single ion channel measurements, substantial noise arises from random statistics of channel entrance. In the chemical reaction problem, the trajectories are not paths of single real particles; rather they describe flux on a complicated potential surface with many degrees of freedom. The simple picture presented in the current paper is not appropriate for either of these phenomena. It does permit, however, an unambiguous computation of the ion flux in biological channels, with concentration boundary conditions.

ACKNOWLEDGMENTS

We thank Abe Nitzan and J. T. Hynes for incisive remarks and very helpful suggestions. The biologist among

TABLE V. The electric current for a typical choice of geometry and concentrations. Note: $I=e\pi r^2 J$, where (Ref. 1) $J=D\{c_L \exp[e\phi(0)/kT]-c_R \exp[e\phi(d)/kT]/\int_0^d \exp[e\phi(\xi)/kT]d\xi\}$ and $r=5$ Å, $c_L=c_R=100$ mM/ℓ, e is the proton charge, I_{cf} is the current derived from a linear potential, constant field theory (Ref. 1) with the same parameters but, of course, without barrier.

Eckart Parameters	Small barrier $A=1$, $B/A=2$	Medium barrier $A=1$, $B/A=6$	Large barrier $A=4$, $B/A=2$	Largest barrier $A=4$, $B/A=6$
I in pA	0.614	0.4039	1.096	0.086
I_{cf} in pA	3.015	3.015	12.059	12.059

us is most grateful to Malgorzata Kłosek and Zeev Schuss for showing him how ionic fluxes are stochastic processes. We are glad for the support of the Department of Energy (ER 13640-4 to M. R.) and the National Science Foundation (DIR 9012294 to R. E.).

APPENDIX: FLUX, CONCENTRATION, AND FIRST-PASSAGE TIME

Consider the first-passage time of an auxiliary problem *different* from the stochastic process of the text, Eq. (2.19) *et seq.*, a problem with the same potential, diffusion constant, and absorbing boundary on the right (at $x=d$), as in the text, but now with a reflecting boundary condition on the left (at $x=0$). If we denote the auxiliary functions (for the process between reflecting and absorbing boundaries) and their moments by tildes to distinguish them from the ones used up to now, then clearly

$$-n\tilde{\mathcal{D}}_{n-1}=D\tilde{\mathcal{K}}'_n+\mu\tilde{\mathcal{K}}_n,$$
$$\tilde{\mathcal{D}}'_n=\tilde{\mathcal{K}}_n, \tag{A1}$$

since the diffusion process is the same. However, the boundary conditions now read

$$\tilde{\mathcal{K}}_n(0)=0,$$
$$\tilde{\mathcal{D}}_n(d)=\delta_{n0}. \tag{A2}$$

Repeating the same steps as previously, we multiply the second equation in Eq. (2.16) by $\tilde{\mathcal{K}}_n(x)$ and integrate over x, namely,

$$\tilde{J}\cdot\int_0^d\tilde{\mathcal{K}}_n(x)dx=-D\tilde{c}\tilde{\mathcal{K}}_n(x)\,|_0^d+\int_0^d\tilde{c}\{-D\tilde{\mathcal{K}}'_n+\mu\tilde{\mathcal{K}}_n\}dx \tag{A3}$$

which, on account of Eq. (A1) can be written as

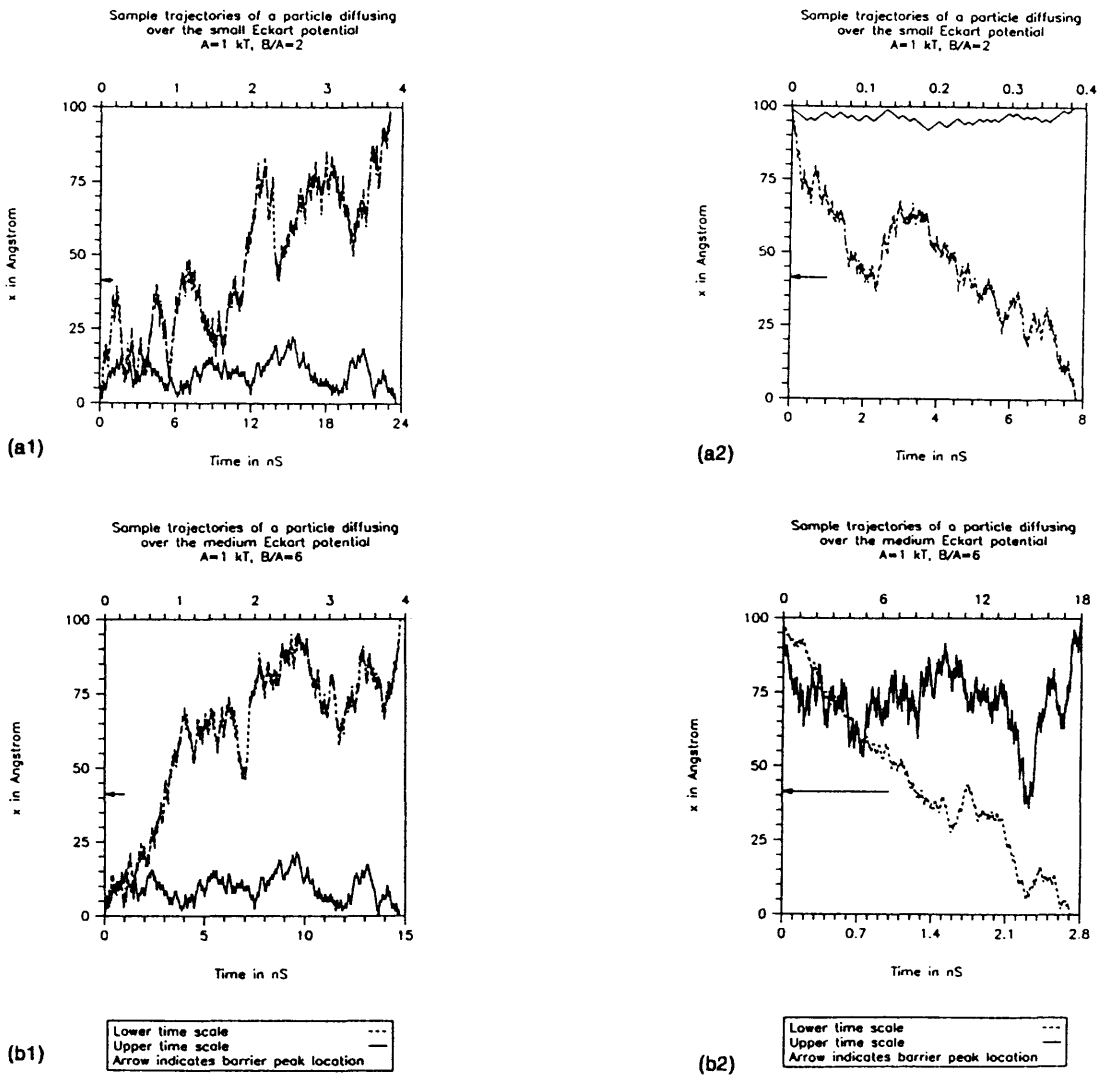

FIG. 5. Characteristic trajectories for diffusing particles, performing random walks, moving over the various choices of Eckart potential. Notice that for relatively small barriers, such as those in (a1), (a2), and (c2), trajectories recross the barrier top fairly commonly; conversely, for very high barriers, such as Fig. (d1), trajectories flow in one direction over the barrier top, although to and fro motions are common in the flat regions of potential.

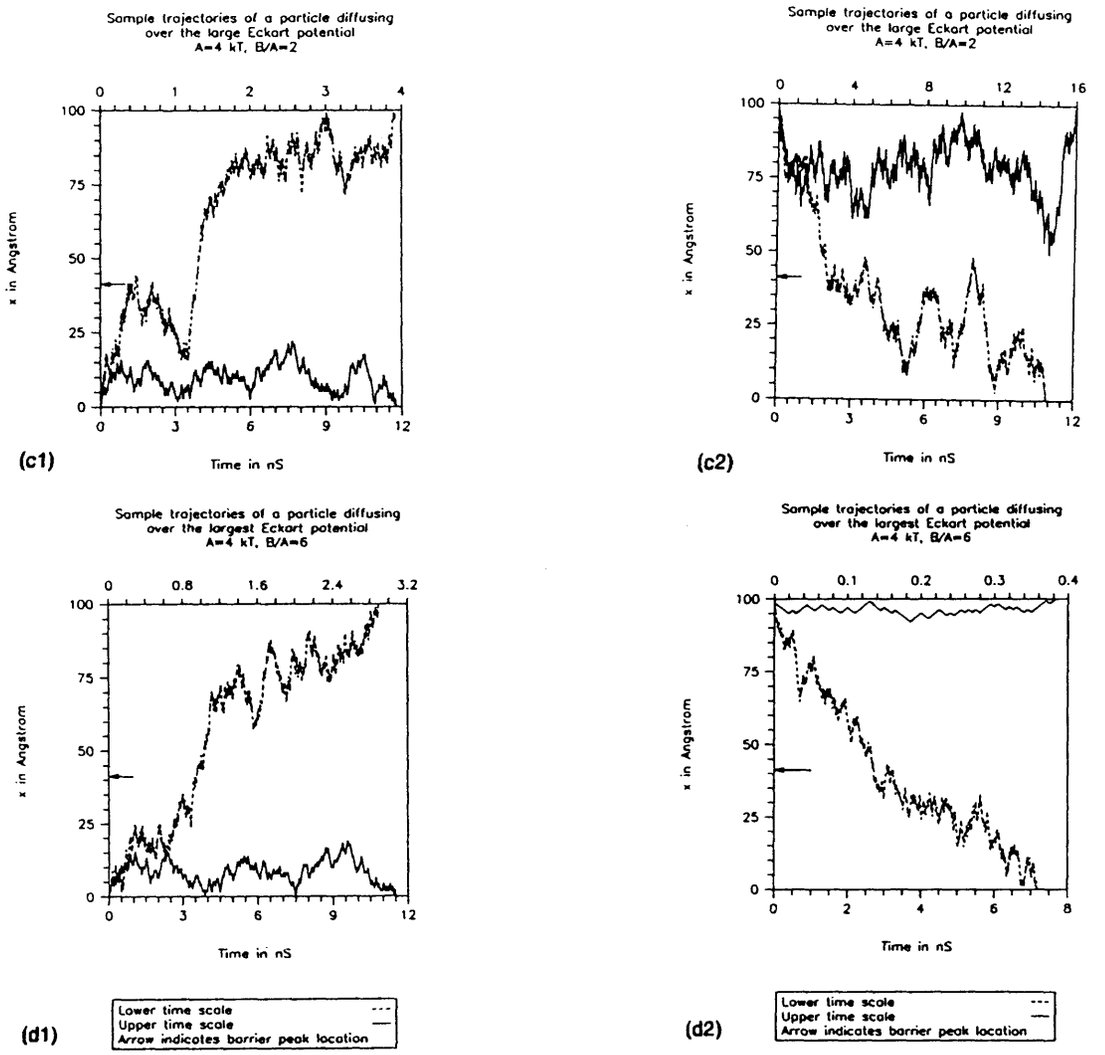

FIG. 5. (*Continued.*)

$$\tilde{J}\cdot\tilde{\mathscr{D}}_n(x)\,|_0^d = -D\tilde{c}\tilde{\mathscr{K}}_n(x)\,|_0^d - n\int_0^d \tilde{c}\tilde{\mathscr{D}}_{n-1}(x)dx. \tag{A4}$$

Select the value $n=1$, then, after making use of the boundary conditions, we deduce that

$$-\tilde{J}\cdot\tilde{\mathscr{D}}_1(0) = -Dc_R\tilde{\mathscr{K}}_1(d) - \int_0^d \tilde{c}(x)\tilde{\mathscr{D}}_0(x)dx. \tag{A5}$$

This expression can be simplified further after establishing that

TABLE VI. The calculation of flux over the Eckart potential by *full Langevin* scheme.

Eckart Parameters	Small barrier $A=1$, $B/A=2$	Medium barrier $A=1$, $B/A=6$	Large barrier $A=4$, $B/A=2$	Largest barrier $A=4$, $B/A=6$
$\mathscr{K}_0(0)_{\text{exact}}$	1.288×10^{-2}	8.464×10^{-3}	1.476×10^{-2}	1.156×10^{-3}
$\mathscr{K}_0(0)_{\text{sim}}$	1.269×10^{-2}	8.559×10^{-3}	1.484×10^{-2}	1.281×10^{-3}
Error in $\mathscr{K}_0(0)$	3%	2%	2%	10%
$\mathscr{K}_0(d)_{\text{exact}}$	4.753×10^{-3}	3.125×10^{-3}	2.744×10^{-4}	2.150×10^{-5}
$\mathscr{K}_0(d)_{\text{sim}}$	4.890×10^{-3}	3.000×10^{-3}	2.818×10^{-4}	2.417×10^{-5}
Error in $\mathscr{K}_0(d)$	2%	4%	4%	12%
N_s^0	5 000	5 000	5 000	5 000
N_f^0	784 180	1 163 570	6 728 801	78 031 250
N_s^d	1 441 430	3 331 090	35 403 040	264 734 490
N_f^d	3 500	5 000	5 000	3 200
Δx	0.5	0.5	0.5	0.5
Δt (pS)	1.0×10^{-3}	1.0×10^{-3}	5.0×10^{-3}	2.0×10^{-2}

$$\tilde{\mathscr{K}}_0(x)=0,$$

$$\tilde{\mathscr{D}}_0(x)=1. \tag{A6}$$

Substituting in Eq. (2.30), we get

$$-\tilde{J}\tilde{\mathscr{D}}_1(0)=-Dc_R\tilde{\mathscr{K}}_1(d)-\int_0^d \tilde{c}(x)dx. \tag{A7}$$

The term $\int_0^d \tilde{c}(x)dx$ is referred to as the "contents" of the channel; $\tilde{\mathscr{D}}_1(0)$ is of course the mean first-passage time for a walker starting at $x=0$ and being absorbed at $x=d$ with a refecting boundary at the left. Therefore, *for the special case* $c_R=0$, the above formula reads

$$\tilde{J}=\frac{\int_0^d \tilde{c}(x)dx}{\tilde{\mathscr{D}}_1(0)}, \tag{A8}$$

i.e., "flux equals contents over mean first-passage time." This relation between steady state flux and mean first passage time has been widely used in the literature. However, the analysis in the text of flux between two absorbing boundaries yields quite different results, see Eqs. (2.24) and (2.20).

[1] D. P. Chen, V. Barcilon, and R. S. Eisenberg, Biophys. J. **61**, 1372 (1992).
[2] K. E. Cooper, E. Jakobsson, and P. G. Wolynes, Prog. Biophys. Mol. Biol. **46**, 51 (1985).
[3] B. Hille, *Ionic Channels of Excitable Membranes*, 2nd ed. (Sinauer, Massachusetts, 1992).
[4] B. Alberts, D. Bray, J. Lewis, M. Raff, K. Roberts, and J. D. Watson, *Molecular Biology of the Cell*, 2nd ed. (Garland, New York, 1989).
[5] V. Barcilon, D. P. Chen, and R. S. Eisenberg, SIAM J. Appl. Math. **52**, 1405 (1992).
[6] P. C. Jordan, Biophys. J. **45**, 1091, 1101 (1984); J. Phys. Chem. **91**, 6582 (1987).
[7] J. T. Hynes, Ann. Rev. Phys. Chem. **36**, 573 (1985); in *Theory of Chemical Reactions*, edited by M. Baer (CRC, Boca Raton, 1986), Chap. 4.
[8] G. R. Fleming, *Chemical Applications of Ultrafast Spectroscopy* (Oxford University, Oxford, 1986); Ann. Rev. Phys. Chem. **37**, 81 (1986); G. R. Fleming, S. H. Courtney, and M. W. Balk, J. Stat. Phys. **42**, 83 (1986).
[9] A. Nitzan, Adv. Chem. Phys. **70**, 489 (1988).
[10] S. A. Adelman, Adv. Chem. Phys. **53**, 61 (1983).
[11] J. N. Onuchic and P. G. Wolynes, J. Phys. Chem. **92**, 6495 (1988).
[12] P. M. Morse and H. Feshbach, *Methods of Theoretical Physics* (McGraw-Hill, New York, 1953), p. 857–860; p. 870ff.
[13] G. H. Weiss, Adv. Chem. Phys. **13**, 1 (1966).
[14] N. S. Goel and N. Richter-Dyn, *Stochastic Models in Biology* (Academic, New York, 1974), p. 60–66.
[15] T. Naeh, M. M. Kłosek, B. J. Matkowsky, and Z. Schuss, SIAM J. Appl. Math **50**, 595 (1990); Lect. Appl. Math. **27**, 241 (1991).
[16] E. B. Nauman and B. A. Buffham, *Mixing in Continuous Flow Systems* (Wiley, New York, 1983).
[17] R. A. Siegel, J. Phys. Chem. **95**, 2556 (1991).
[18] M. Rubinovitch and U. Mann, AICHE J. **29**, 658 (1983).
[19] D. R. Cox and H. D. Miller, *The Theory of Stochastic Processes* (Chapman and Hall, London, 1965).
[20] G. H. Weiss and R. J. Rubin, Adv. Chem. Phys. **52**, 363 (1983).
[21] M. E. Widder and U. M. Titulaer, Physica A **154**, 452 (1989).
[22] N. G. Van Kampen, *Stochastic Processes in Physics and Chemistry* (North-Holland, New York, 1981); J. Phys. Chem. Solids **49** 673 (1988); IBM J. Res. Dev. **32**, 107 (1988); J. Math. Phys. **29**, 1220 (1988).
[23] I. Dayan, and G. H. Weiss, J. Chem. Phys. **92**, 5235 (1990).
[24] M. Kac, Rocky Mountain J. Math. **4**, 497 (1974).
[25] L. Arnold, *Stochastic Differential Equations: Theory and Applications* (Wiley, New York, 1973).
[26] Z. Schuss, *Theory and Applications of Stochastic Differential Equations* (Wiley, New York, 1980).
[27] T. C. Gard, *Introduction to Stochastic Differential Equations* (Marcel Dekker, New York, 1988).
[28] H. Lamb, *Hydrodynamics* (Dover, New York, 1945), p. 2ff; G. K. Batchelor, *An Introduction to Fluid Dynamics* (Cambridge University, New York, 1976), p. 71ff.
[29] C. W. Gardiner, *Handbook of Stochastic Methods: For Physics, Chemistry and the Natural Sciences* (Springer, New York, 1983).
[30] S. Chandrasekhar, Rev. Mod. Phys. **15**, 1 (1943).
[31] E. Nelson, *Dynamic Theories of Brownian Motion* (Princeton University, Princeton, 1967).
[32] J. Kevorkian and J. D. Cole, *Perturbation Methods in Applied Mathematics* (Springer, New York, 1967).
[33] H. Risken, *The Fokker–Planck Equation: Methods of Solution and Applications* (Springer, New York, 1984).
[34] J. L. Skinner and P. G. Wolynes, J. Chem. Phys. **72**, 4913 (1980).
[35] D. G. Truhlar, W. L. Hase, and J. T. Hynes, J. Phys. Chem. **87**, 2664 (1983); B. C. Garrett, and D. G. Truhlar, *ibid.* **84**, 682(E) (1980); E. Pollak, J. Chem. Phys. **86**, 3944 (1987); R. E. Cline and P. G. Wolynes, *ibid.* **86**, 3836 (1987).
[36] H. A. Kramers, Physica 7, 284 (1940).
[37] T. Fonseca, J. A. N. F. Gomes, P. Grigolini, and F. Marchesoni, Adv. Chem. Phys. **62**, 389 (1985).
[38] K. Schulten, Z. Schulten, and A. Szabo, J. Chem. Phys. **74**, 4426 (1981).
[39] B. J. Matkowsky, Z. Schuss, and C. Tier, J. Stat. Phys. **35**, 443 (1984).
[40] E. Pollak, J. Chem. Phys **85**, 865 (1986).
[41] P. Hanggi, P. Talkner, and M. Borokovec, Rev. Mod. Phys. **62**, 251 (1986).
[42] B. Carmeli and A. Nitzan, Phys. Rev. A **29**, 1481 (1984); J. Chem. Phys. **80**, 3596 (1984); Chem. Phys. Lett. **106**, 329 (1984).
[43] C. Eckart, Phys. Rev. **25**, 1303 (1930); D. Rapp, *Quantum Mechanics* (Holt, Rinehardt, and Winston, New York, 1971).
[44] B. Roux, and M. Karplus, J. Phys. Chem. **95**, 4856 (1991); S. W. Chiu and E. Jakobsson, Biophys. J. **61**, A524 (1992).
[45] B. Roux, and M. Karplus, Biophys. J. **59**, 961 (1991).
[46] M. A. Ratner, Acc. Chem. Res. **15**, 355 (1982); R. Rosenberg, Y. Boughaleb, A. Nitzan, and M. A. Ratner, Solid State Ionics **18**, 127 (1986); **19**, 160 (1986); M. A. Ratner, Polymer Electrolyte Rev. **1**, 173 (1987).
[47] K. E. Cooper, P. Y. Gates, and R. S. Eisenberg, Quart. Rev. Biophys. **21**, 331 (1988); J. Membr. Biol. **109**, 95 (1988).
[48] E. Jakobsson and S. W. Chiu, Biophys. J. **52**, 33 (1987).
[49] P. Y. Gates, K. E. Cooper, and R. S. Eisenberg, *Ion Channels*, edited by T. Narahashi (Plenum, New York, 1990), Vol. 2, pp. 233–281; P. Y. Gates, K. E. Cooper, J. Rae, and R. S. Eisenberg, Prog. Biophys. Mol. Biol. **53**, 153 (1989).
[50] S. A. Adelman, and J. D. Doll, J. Chem. Phys. **64**, 2375 (1976).
[51] J. Schroeder, D. Schwarzer, J. Troe, and F. Voss, J. Chem. Phys. **93**, 2393 (1990).
[52] N. Agmon, and R. Kosloff, J. Phys. Chem. **91**, 1988 (1987).
[53] R. F. Grote, and J. T. Hynes, J. Chem. Phys. **74**, 4465 (1981).
[54] S. A. Adelman, J. Stat. Phys. **42**, 37 (1986).
[55] M. M. Kłosek-Dygas, B. M. Hoffman, B. J. Matkowsky, A. Nitzan, M. A. Ratner, and Z. Schuss, J. Chem. Phys. **90**, 1141 (1989); **95**, 1425 (1991).
[56] N. Agmon and J. J. Hopfield, J. Chem. Phys. **78**, 6947 (1983); **79**, 2042 (1983).
[57] B. M. Hoffman and M. A. Ratner, J. Am. Chem. Soc. **109**, 6237 (1987); **110**, 8267 (1988).
[58] C. Gehrke, J. Schroeder, D. Schwarzer, J. Troe, and F. Voss, J. Chem. Phys. **92**, 4805 (1990).
[59] M. M. Dygas, B. J. Matkowsky, and Z. Schuss, SIAM J. Appl. Math. **46**, 265 (1986).
[60] Z. Schuss and B. J. Matkowsky, SIAM J. Appl. Math. **35**, 604 (1979); B. Gaveau, J. T. Hynes, R. Kapral, and M. Moreau, J. Stat. Phys. **56**, 879 (1989).
[61] T. H. Forster and G. Hoffman, Z. Phys. **75**, 63 (1971).

[62] B. Bagchi, D. W. Oxtoby, and G. R. Fleming, J. Chem. Phys. **86**, 257 (1984).
[63] D. G. Levitt, Biophys. J. **37**, 575 (1982).
[64] S. W. Chiu and E. Jakobsson, Biophys. J. **55**, 147 (1989).
[65] D. G. Levitt, Ann. Rev. Biophys. Chem. **15**, 29 (1986).
[66] W. Dieterich, P. Fulde, and I. Peschel, Adv. Phys. **29**, 527 (1980).
[67] S. H. Jacobson, M. A. Ratner, and A. Nitzan, J. Chem. Phys. **78**, 4154 (1983).